Maturation of the infant respiratory microbiota, environmental drivers and health consequences: a prospective cohort study

Title: Maturation of the infant respiratory microbiota, environmental drivers and health consequences: a prospective cohort study

Authors: Astrid A.T.M. Bosch[1,2†], Wouter A.A. de Steenhuijsen Piters[1,3,4†], Marlies A. van Houten[2], Mei Ling J.N. Chu[1,3], Giske Biesbroek[1,2], Jolanda Kool[5], Paula Pernet[6], Pieter-Kees C.M. de Groot[6], Marinus J.C. Eijkemans[7], Bart J.F. Keijser[5,8], Elisabeth A.M. Sanders[1] and Debby Bogaert[1,3,4*]

† These authors contributed equally to this work.

* Corresponding author. Email: D.Bogaert@ed.ac.uk. Telephone: 0131 242 6582.

Affiliations

[1] Department of Paediatric Immunology and Infectious Diseases, Wilhelmina Children's Hospital/University Medical Center Utrecht, Lundlaan 6, 3584 EA, Utrecht, The Netherlands.

[2] Spaarne Gasthuis Academy, Spaarnepoort 1, 2134 TM Hoofddorp, The Netherlands.

[3] Department of Medical Microbiology, University Medical Center Utrecht, Heidelberglaan 100, 3584 CX Utrecht, The Netherlands.

[4] Medical Research Council/University of Edinburgh Centre for Inflammation Research, Queen's Medical Research Institute, University of Edinburgh, 47 Little France Crescent, EH16 4TJ Edinburgh, United Kingdom.

[5] Microbiology and Systems Biology Group, Netherlands Organisation for Applied Scientific Research (TNO), Utrechtseweg 48, 3704 HE Zeist, The Netherlands.

[6] Department of Obstetrics and Gynaecology, Spaarne Gasthuis, Spaarnepoort 1, 2134 TM Hoofddorp, The Netherlands.

[7] Biostatistics and Research Support, Julius Center for Health Sciences and Primary Care, University Medical Center Utrecht, Universiteitsweg 100, 3584 CG Utrecht, The Netherlands.
[8] Department of Preventive Dentistry, Academic Center for Dentistry Amsterdam (ACTA), University of Amsterdam and Vrije University Amsterdam, Gustav Mahlerlaan 3004, 1081 LA Amsterdam, The Netherlands.

Author contributions

MAvH, EAMS, and DB designed the experiments, AATMB, MAvH, GB, EAMS, and DB wrote the study protocols. AATMB, PP and PCMdG were responsible for patient recruitment. AATMB and MAvH were responsible for clinical data collection. MLC was responsible for sample preparation and MLC, JK, and BK for 16S-rRNA gene amplicon sequencing. WAAdSP, MJCE and DB were responsible for bioinformatic processing and statistical analyses. WAAdSP, AATMB, and DB wrote the paper. All authors significantly contributed to interpreting the results, critically revised the manuscript for important intellectual content, and approved the final manuscript.

Funding

This work was supported in part by The Netherlands Organisation for Health Research and Development (ZonMW; grant 91209010); The Netherlands Organisation for Scientific research (NWO-VIDI; grant 91715359); Wilhelmina Children's Hospital and Spaarne Gasthuis Hoofddorp intramural funds; and Topconsortia for knowledge and innovation (Agri & Food; TKI-AF-12190).

Running title: Early-life respiratory microbiota development related to infections

Descriptor: 10.11 Pediatrics: Respiratory Infections

Total word count: 4,483/3,500 words**.**

Word count abstract: 260/250 words.

At a glance commentary

What is the current scientific knowledge on this subject?

Factors affecting the risk of respiratory tract infections have been well characterized, however it is unknown how these factors might impact respiratory microbiota development and thereby susceptibility to respiratory tract infections (RTIs). Studies in mice suggest that timely microbial cues contribute to healthy immune development, in turn enforcing the defense against invading respiratory pathogens.

What does this study add to the field?

Using a longitudinal study design and high sampling resolution, we characterized the nasopharyngeal microbiota maturation over the first year of life in 112 infants both during health (11 sampling moments) and at the moment of RTIs. We observed differences in the microbial community maturation in children who ultimately became more susceptible to infections compared to children who were more resistant to infections. These changed dynamics were related to shifts in the abundance of specific members of the microbiota and environmental factors that are known to impact susceptibility to RTIs, such as mode of delivery, mode of feeding, early antibiotic use and crowding. Altered microbiota maturation was evident from the first month of life on and preceded factual RTIs, strongly suggesting that early-life microbiota development impacts long-term respiratory health.

This article has an online data supplement, which is accessible from this issue's table of content online at www.atsjournals.org

Abstract

Rationale: Perinatal and postnatal influences are presumed important drivers of the early-life respiratory microbiome composition. We hypothesized that the respiratory microbiome composition and development in infancy is affecting microbiome stability and thereby resilience against respiratory tract infections (RTIs) over time.

Objectives: To investigate common environmental drivers, including birth mode, feeding type, antibiotic exposure and crowding conditions, in relation to respiratory tract microbiota maturation and stability, and consecutive risk of RTIs over the first year of life.

Methods: In a prospectively followed cohort of 112 infants, we characterized the nasopharyngeal microbiota longitudinally from birth on (11 consecutive sample moments and maximum three RTI samples per subject; in total *n*=1,121 samples) by 16S-rRNA gene amplicon sequencing.

Measurements and Main Results: Using a microbiota-based machine-learning algorithm we found that children experiencing a higher number of RTIs in the first year of life demonstrate an aberrant microbial developmental trajectory already from the first month of life on as compared to the reference group (0-2 RTIs/year). The altered microbiota maturation process coincided with decreased microbial community stability, prolonged reduction of *Corynebacterium* and *Dolosigranulum*., enrichment of *Moraxella* already very early in life, followed by later enrichment of *Neisseria* and *Prevotella* spp. Independent drivers of these aberrant developmental trajectories of respiratory microbiota members were mode of delivery, infant feeding, crowding and recent antibiotic use.

Conclusions: Our results suggest that environmental drivers impact microbiota development and consequently resilience against development of RTIs. This supports the idea that microbiota form the mediator between early life environmental risk factors for and susceptibility to RTIs over the first year of life.

106 **Key words:** respiratory microbiota, nasopharynx, respiratory tract infections, development,
107 risk factors.
108

Introduction

Acute respiratory tract infections (RTI) are a leading cause of childhood mortality, being responsible for ~0.9 million yearly deaths (15.5% of all deaths) worldwide in children <5 years (1). In addition, these infections are associated with significant morbidity (2) and are a major reason for antibiotic prescription (3), especially in young children. Although it is still unclear why one individual is more vulnerable to respiratory infections compared to another, it was previously hypothesized that - besides environmental and host-related influences - the respiratory microbiota may modulate susceptibility to disease.

Directly after birth, the mucosal surfaces of the respiratory tract of neonates are rapidly colonized with a variety of microbiota, that are swiftly moulded into niche-specific bacterial communities (4, 5). Over the first months to years of life, these communities are highly dynamic and heavily influenced by environmental factors, including mode of delivery (4, 6), season (7), feeding type (8), and antibiotic treatment (9). In previous studies we found that the microbial composition at the age of six weeks was indicative of microbiota stability and RTI susceptibility over the first two years of life (10, 11). This finding underscores the importance of direct postnatal environmental influences and subsequent early microbiota maturation on future respiratory health.

The healthy human respiratory microbiome is assumed to stimulate immune maturation (12, 13), promote epithelial integrity (14), and provide colonization resistance (15), thereby preventing overgrowth and invasion of potential pathogenic bacteria (16). In contrast, deviations from a healthy bacterial respiratory community composition have been associated with susceptibility to and/or severity of childhood respiratory diseases, including acute otitis

media (17, 18), respiratory syncytial virus (RSV) disease (19) and asthma development (20) in various retrospective and cross-sectional studies (21).

We here postulate that alterations in the respiratory microbiome development early in life are a consequence of changes in the abundance of specific bacterial biomarkers species. We hypothesize that these alterations are controlled by known host-related and environmental influences, and can ultimately lead to altered microbiota stability, in turn affecting RTI susceptibility. Therefore, we prospectively investigated the nasopharyngeal microbiota maturation of 112 unselected, healthy children with frequent, short interval sampling during the first year of life as well as during RTI episodes. Hereby, we aimed to study respiratory microbiota development early in life, and investigate its role as potential mediator between early-life drivers and susceptibility to respiratory infectious disease.

Methods

Details on the study design, sample and data collection and bioinformatics/statistical methods can be found in the online supplement Methods. Data have been deposited in the National Center for Biotechnology Information GenBank database (accession number: SRP093519).

Study population

We enrolled in total 128 healthy children in an ongoing prospective birth cohort study aiming to investigate the development of the infant microbiome during health and disease. Of 128 infants, 12 children were lost to follow-up (Figure E1). Details on the trial methods have been described elsewhere (4). Written informed consent was obtained from both parents. The study

was approved by the Ethics Committee of Noord Holland, The Netherlands (M012-015, NH012.394, NTR3986). Sequence data of part of the samples (≤6 months; n=743 samples of 101 children) were used for a study on the role of mode of delivery on respiratory microbiota acquisition (4).

Data collection

For the current analyses, we included samples and data of 112/116 children who completed the one-year follow-up and for whom we had ≥8 samples available for further analyses after laboratory work-up (Figure E1). Home visits were conducted within two hours after birth, at 24 hours, at seven and 14 days, and at one, two, three, four, six, nine, and 12 months of age. During each home visit, a trained doctor or research nurse obtained a nasopharyngeal swab according to World Health Organization protocol (22) and completed an extensive survey on the health status of the child, as well as on the presence or absence of potential risk and environmental factors related to respiratory disease (4). Next to these regular visits, parents were asked to contact the study team in case of an active RTI, defined as fever ≥38°C for >6 hours combined with malaise and presence of RTI symptoms. Following, a RTI visit was planned within 48 hours after start of the fever to collect additional samples and to obtain more detailed medical information.

16S-rRNA gene amplicon sequencing

Bacterial DNA of the nasopharyngeal samples was isolated, amplicon libraries of the 16S-rRNA gene (V4 region) were generated, and sequencing was executed as previously described (4, 23). Amplicon pools were paired-end sequenced in eight runs using an Illuminia MiSeq instrument (Illumina Inc., San Diego, CA, USA). Bioinformatic processing included trimming, error correction, assembly and 97%-identity clustering of reads into OTUs. Following removal

of chimeric reads, OTUs were taxonomically annotated using SILVA and BLASTN (Table E1). We refer to OTUs using maximum genus level annotations, combined with a rank number based on the abundance of each given OTU. Details on processing and quality control, including the use of negative controls, are described in the online supplement Methods. After abundance-filtering, a rarefied dataset was generated, and used for downstream analyses (24). α-diversity measures were averaged over 100 rarefactions. β-diversity was assessed using the Bray-Curtis dissimilarity metric.

Statistical analysis

All analyses were performed in the R version 3.3.0 within R studio version 0.99.902.

Random forest analysis

We hypothesized that the nasopharyngeal microbial succession patterns would be altered in children who experienced more RTIs during their first year of life. Therefore, we stratified our population into three groups based on the normal distribution of RTIs over the first year of life (Figure E2); 39 children with 0-2 RTIs (reference group; *n*=372 samples), 52 children with 3-4 RTIs (*n*=496 samples) and 21 children with 5-7 RTIs (*n*=197 samples). To identify OTUs characteristic of a healthy microbiota maturation, we regressed the relative abundance of all 576 OTUs against chronological age in the reference group using the *randomForest* package, and selected age-discriminatory OTUs using a step-wise backward 10-fold cross validation procedure, see online supplement Methods and Figure E3A and E3B (24). This selection of OTUs was subsequently used as input to a random forest model where we regressed the relative abundance of these OTUs versus chronological age in the reference group. The resulting final model was then used to predict chronological age, referred to as 'microbiota age', in samples from individuals who experienced 3-4 and 5-7 RTIs and on the group of samples collected

during RTIs (*n*=56 samples). To generate accurate microbiota age estimates for the reference group, we used a 10-fold cross-validation procedure. Relative microbiota age (RMA) was calculated as follows: relative microbiota age = microbiota age of a given child – microbiota age of the reference group at similar age as determined by a spline fit (24). As a post-hoc analysis, we studied the effect of the *Moraxella*-genus on the performance of the microbiota age model by excluding the OTUs belonging to the *Moraxella*-genus from the model while monitoring the amount of variance explained.

Associations between environmental factors and microbiota parameters

'Environmental factors' used in the descriptions of the various models comprises birth mode, breast feeding until three months of age, day care attendance, presence of siblings >five years of age, antibiotic treatment in the previous four weeks and season of birth, if not specified otherwise. If applicable, correction for multiple testing was performed using the Benjamini-Hochberg procedure.

Microbial succession patterns were visualised using non-metric multidimensional scaling (nMDS; *vegan* package) based on the Bray-Curtis dissimilarity matrix. We performed two separate analyses based on permutational multivariate analysis of variance (PERMANOVA)-tests and the Bray-Curtis dissimilarity matrix, to study the effect of 1) environmental factors, age and subject, and 2) the number of RTIs experienced in the first year of life, on the overall bacterial community structure. Permutations were constrained within subjects to account for repeated measures. This analysis was repeated over 100 rarefactions to assess the robustness of our results based on one rarefied set.

To complement the group-based analyses, we also assessed the microbial development at the individual level using an unsupervised clustering approach. The proportion of samples within each cluster at each time point was visualised using an alluvial diagram, stratified by the number of RTIs that children experienced over the first year of life.

We used separate linear mixed models to assess the associations between (relative) microbiota age and stability (α-/β-diversity measures) as dependent variables and 1) environmental factors and 2) the number of RTIs (fixed effects), while adjusting for age and with the subject-variable included as a random intercept (*lme4* package). In addition, the relationships between 1) bacterial density and 2) relative abundance (dependent) and sampling moment (fixed) were assessed using linear mixed models.

We used smoothing spline analysis of variance (SS-ANOVA; *metagenomeseq* package) for the analyses of 1) the differences in abundance of age-discriminatory OTUs between RTI-groups, and 2) the effects of birth mode and breastfeeding on the nasopharyngeal microbiota, as it simultaneously tests for the existence and timing of differences in OTU-abundance. To confirm associations between environmental factors and relative abundance of microbiota in a multivariable manner, we used the Multivariate Association with Linear Models (MaAsLin) (R-)package, adjusting for age and with subject as a random effect.

Results

Baseline characteristics of the study population

Baseline characteristics of the study population stratified by number of RTIs experienced in the first year of life can be found in Table E2.

Nasopharyngeal microbiota composition in the first year of life

A median of 20,670 reads were generated per sample (range 3,911-97,870 reads), which were binned into a total 576 operational taxonomic units (OTUs; after filtering), representing a total of 14 bacterial phyla. Firmicutes was the most abundant phylum with a maximum abundance of 65.4% at day one (mainly *Staphylococcus (3)*, *Dolosigranulum (4)* and *Streptococcus (5)*). Later, Proteobacteria emerged and became predominant with a maximum abundance of 71.7% at 12 months of life (mostly *Moraxella (1)*, *Haemophilus (6)* and *Moraxella (7)*; Figure 1, Figure 2 and Figure E4). We observed major shifts in nasopharyngeal microbiota composition between day 0 and day one and between day one and week one (Figure E5). The difference in microbiota composition between day one and week one coincided with a strong increase in absolute bacterial abundance, which then increased up to the age of ~1 month, after which it stabilized (linear mixed model; $q<0.001$; Figure 3).

Trajectories of microbial development

We aimed to study whether nasopharyngeal microbiota development is different in infants experiencing more RTIs in the first year of life compared to the low-burden infants. First, we demonstrated that the microbial community composition was significantly associated with the number of RTIs experienced in the first year of life (i.e. 1-7 RTIs; categorical), after adjusting for age, using a PERMANOVA-test (Table E3A; 1.7% of the variance explained, $p=0.001$). Subsequently, we stratified the study participants over three groups based on the number of RTIs they experienced within the first 12 months of life (i.e. 0-2, 3-4 and 5-7 RTIs; Figure E2 and Table E2). To explore the microbial succession patterns at the individual level, we clustered samples using an unsupervised clustering approach. The proportion of individuals in each cluster at each time point was then visualised using an alluvial diagram stratified by the number of RTIs experienced over the first year of life (figure E6). We identified 8 clusters over all time points, of which the largest four were enriched for *Moraxella (1)* (MOR1, 38.5% of samples)

Corynebacterium (2) and *Dolosigranulum (4)* (CDG, 19.7%), *Staphylococcus (3)* (STA, 19.4%) and *Streptococcus (5)* (STR, 8.4%). In concordance with our previous observations, we found that the CDG-cluster has a much more prominent and prolonged role in the reference group compared to children who suffered from 5-7 RTIs. Instead, these children appear to 'skip' the CDG-cluster altogether, transitioning directly from the early-life STA-cluster to the MOR1-cluster (figure E6C), the latter of which is typically observed more often at later time points in the reference cohort (figure E6A). In the children who experience 3-4 RTIs the cluster distributions at each time point do resemble those of the reference group, although an early rise of the *Haemophilus (6)* (HAE)-cluster was noted (figure E6B).

Nasopharyngeal microbiota maturation in relation to susceptibility to RTI and identification of age-discriminatory taxa

To further assess these differences in microbiota dynamics we used a random forest regression model. First, we identified age-discriminatory OTUs in the reference group (i.e. 0-2 RTIs; Figure E3A and 3B) and regressed their relative abundance against chronological age, enabling us to model healthy microbiota development (65.9% of variance explained, based on 10-fold cross-validation, 100 repetitions). Then, the model was used to calculate predicted chronological age or 'microbiota age' in children with 3-4 and 5-7 RTIs and in samples taken during RTIs (58.1% variance explained), subsequently comparing these estimates to chronological age. We first observed that children with 5-7 RTIs showed an accelerated microbiota maturation when compared to the reference group from very early in life on (linear mixed model; p=0.007). A similar, although non-significant trend was observed in children with 3-4 vs reference group (linear mixed model; p=0.13; Figure 4A). The accelerated microbiota developmental patterns in children with >2 RTIs were related to an early enrichment of *Moraxella (1)* from just after birth on (SS-ANOVA; q=0.007), enrichment of *Neisseria*,

297 *Prevotella* and *Alloprevotella* spp. from month two onwards (SS-ANOVA; q≤0.021) and
298 (prolonged) absence of *Corynebacterium (2)* and *Corynebacterium (80)*, *Dolosigranulum (4)*
299 and *Streptococcus (10)* (SS-ANOVA; q≤0.039; Figure 4B, Figure E7 and Table E4A).
300 Subgroup analyses comparing either the 3-4 or 5-7 RTI groups to the reference group yielded
301 highly similar results (Table E4B and E4C).

302 To assess whether the above differences were predominantly driven by the *Moraxella* genus
303 rather than by the total group of biomarkers species, we assessed the impact of *Moraxella* spp.
304 on the performance of the microbiota age model by repeating the analyses including all
305 biomarker OTUs, except those belonging to the *Moraxella*-genus. This model, containing 18
306 OTUs, showed a confined effect of *Moraxella* spp., with a small reduction of performance in
307 the reference group (60.9% variance explained) and a slightly improved performance in
308 children who experienced 3-4 or 5-7 RTIs over the first year of life and in samples taken during
309 RTI (60.1% variance explained), compared with the model based on 22 OTUs.

310 *Relative microbiota age in relation to (susceptibility to) RTI*

311 By calculating the relative microbiota age (RMA; defined as the difference in microbiota age
312 between susceptible groups versus the reference group) we verified that microbiota age was
313 increased in children with 5-7 RTIs compared to the reference group (linear mixed model,
314 adjusted for age; p=0.007; Figure E8), which was already apparent in the first month of life
315 (p=0.011; linear mixed model; post-hoc analysis in children ≤1 month of age). This latter
316 finding was substantiated by a PERMANOVA-test, demonstrating that the microbiota
317 composition over the first month of life was significantly associated with the number of RTIs
318 over the first year of life (Table E3D; 0.8% of the variance explained, p=0.001). The RMA was
319 not significantly different between the group with 3-4 RTIs and the reference group (p=0.12).
320 Moreover, although the RMA was maximal during RTIs (median RMA +67.8 days in RTI

samples), we already observed an increase in RMA during the period preceding the factual RTI (median RMA +37.1 days at the first time point preceding RTI [T = -1]; p=0.004), suggesting that the microbiota maturation alterations precede RTIs. After recovery from an RTI, RMA decreased towards the reference group, though did not normalize (median RMA +29.7 days T = +1; p=0.04; Figure 4C). Although these changes in RMA appeared to be related to individual OTUs (figure E9), these changes were not statically significant.

Nasopharyngeal microbiota stability over time

We next investigated whether bacterial community stability over time was different for children who experienced 0-2, 3-4 and 5-7 RTIs over the first year of life. Community stability, measured by the Bray-Curtis dissimilarity between consecutive time points, was significantly different between children with 0-2 RTIs and those with 3-4 and 5-7 RTIs (linear mixed model; p=0.005 and p=0.02, respectively). This phenomenon was apparent from the age of three months on (Figure 5).

Impact of environmental drivers on bacterial community composition

We then aimed to assess the effect of environmental factors on nasopharyngeal microbiota composition and succession. Using PERMANOVA tests, we found that factors with the largest impact comprised subject (unadjusted R^2=18.7%), chronological age (10.4%) and environmental drivers, including presence of siblings <five years of age (1.6%), day care attendance (0.9%), season of birth (0.7%), breastfeeding for at least three months (0.5%), birth mode (0.4%) and antibiotic usage in the previous month (0.3%; all p-values ≤0.016; Table E3B and E3C).

Environmental drivers and their effects on microbiota maturation, stability and individual bacterial taxa

After showing microbiota maturation is accelerated in children more susceptible to RTIs, we next set out to determine the influence of environmental drivers on this process. We modelled the RMA using a linear mixed model including environmental factors. We observed that particularly the presence of young siblings and day care attendance are associated with an increased RMA early in life (both $p<0.0005$). Similar associations were found when directly modelling microbiota age instead of RMA versus environmental drivers (data not shown). In contrast, the observed differences in microbiota stability between groups could not be explained by environmental factors (linear mixed model; $p>0.05$) and did not relate to differences in α-diversity measures between groups (linear mixed model; $p>0.05$, Figure E10). We also did not detect differences in microbiota stability directly prior to, during or following a RTI episode.

We further tested the contribution of individual bacterial taxa to the associations between environmental factors and microbiota maturation using MaAslin. With respect to age-discriminatory taxa, we found that *Moraxella* spp. were positively and *Staphylococcus* spp. were negatively associated with day care (both $q<0.0005$). Furthermore, we found that *Corynebacterium (2)* and *Dolosigranulum (4)* were strongly reduced following antibiotic usage ($q<0.03$). Additionally, we observed many associations between environmental drivers and bacterial taxa that were not previously assigned as age-discriminatory biomarkers. Notably, the presence of siblings was associated with increased abundance of the family *Pasteurellaceae* ($q=0.003$), which includes the *Haemophilus* genus (Table E5).

Temporal effects of mode of delivery and feeding type on bacterial taxa

Since MaAsLin is not suited to identify temporary effects and the timeframes within which they occur, we additionally studied the impact of early life drivers, such as mode of delivery and feeding type, on the microbial succession patterns using SS-ANOVA. Of the age-discriminatory taxa, early and/or prolonged predominance of *Corynebacterium (2)*,

Corynebacterium (8) and *Dolosigranulum (4)* ($q \leq 0.03$) and late enrichment of *Moraxella* spp. ($q < 0.05$; from ~month 3 on) were associated with vaginal birth and/or breastfeeding. Contrariwise, in formula fed and/or caesarian born children we observed a high abundance of *Gemella (9)* and *Streptococcus (10)* ($q \leq 0.012$) from birth on, and prolonged (4-11 months) predominance of *Neisseria* spp. and (facultative) anaerobes including *(Allo)prevotella*, *Granulicatella* and *Actinomyces* spp. ($q < 0.05$) after the first month of life. Abundance of the age-discriminatory taxum *Staphylococcus (3)* was related to birth by caesarian section in the first month of life only ($q = 0.016$). Besides, although not directly linked to microbiota maturation, we found that the additional early enrichment of *Streptococcus (5)* was associated with caesarian section and/or formula feeding (from birth on; $q \leq 0.026$), which could be confirmed using MaAsLin (Table E5). Additionally, we observed temporal enrichment of oral type of bacteria including streptococci and facultative anaerobic bacteria like *Prevotella*, *Porphyromonas* and *Veillonella* spp., in formula fed children (from ~month 1-2 onwards) and early abundance of *Dolosigranulum (4)* in breastfed children (Table E6 and E7 and Figure E11 and E12).

Discussion

Microbial colonization of the upper respiratory tract occurs directly after birth and develops rapidly towards niche-specific profiles during the first weeks of life (4, 5, 10, 25). Several cross-sectional case-control studies have shown differences in respiratory microbial profiles between children with and without acute otitis media (18, 26), and between infants with mild, moderate and severe RSV (19). Longitudinal studies, linking respiratory microbiota development and

391 maturation and (risk of) RTIs, however, are sparse, lack detailed information, and are only
392 retrospectively executed (10, 20).
393
394 Our results suggest that microbiota maturation in healthy children who experience a limited
395 number of 0-2 RTIs in the first year of life (reference group), is associated with a specific timing
396 of colonization events accompanied by the consecutive appearance and disappearance of
397 specific community members. In general, we observed that during the first week of life, the
398 microbiota development is typified by a strong increase in absolute bacterial abundance. In the
399 reference group, this coincides with the initial expansion of *Streptococcus* spp. at day one,
400 supplanted by rapid niche-differentiation at one week of life, initially driven by staphylococcal
401 predominance, but quickly followed by the establishment of multiple *Corynebacterium* and
402 *Dolosigranulum* spp.: a process which is strongly related to vaginal delivery (4) as well as
403 breastfeeding. Although *Moraxella* spp. become predominant community members over time
404 in most children, in the reference group they only become the main community members from
405 2-3 months of life on. From that age on, *Moraxella* spp. may still co-occur with
406 *Corynebacterium* and *Dolosigranulum* spp. in a mixed community profile or they can truly
407 dominate all other community members in a *Moraxella* spp. dominated community profile (4).
408 This natural process of consecutive events coincides with normalization of ecological stability
409 from the age of three months on and fewer infections.
410 In contrast, children with high susceptibility to RTIs over the first year of life exhibit an
411 accelerated bacterial community maturation from as early as the first month of life on, i.e. prior
412 to development of their first RTIs. This pattern was characterised by diminished and less
413 prolonged establishment of *Corynebacterium* and *Dolosigranulum* spp. coinciding with
414 premature predominance of *Moraxella* spp. colonization, and more abundant and prolonged
415 presence of oral types of bacteria in the nasopharyngeal niche, including *Neisseria* and

Prevotella spp. The observed aberrant microbial succession in children with more RTIs also coincided with decreased bacterial community stability over time, which is in line with previous observations and support the ecological theory that more stable microbiota are more resistant to RTIs (10). Interestingly, we could also show that acceleration of microbiota age preceded the factual RTIs, supporting the hypothesis that microbiota changes forego a clinically symptomatic RTI. Conjointly, these findings support our hypothesis that the initial early colonization after birth and subsequent development of URT microbiota over the first months of life impact respiratory health.

Our data, in line with others, show that prolonged abundance of *Corynebacterium* and *Dolosigranulum* spp. are linked to healthy microbiota development and microbiota stability (10, 17, 20, 26), and are related to breastfeeding and vaginal delivery (4, 8, 27). Their co-occurrence may be explained by the ability of *Dolosigranulum* spp. to produce lactic acid, which plausibly selects for *Corynebacterium* spp. outgrowth (21). Antagonism between *Corynebacterium* spp., and *Streptococcus pneumoniae*, a known respiratory pathogen, may at least in part explain their association with respiratory health (17, 26, 28). Since we and others (20, 29) showed that antibiotic use in infancy is associated with depletion of *Corynebacterium* and *Dolosigranulum* spp., routinely used antibiotics may therefore have more (prolonged) consequences for microbiota-driven resilience against RTIs than currently is thought.

Conversely, accelerated microbial succession patterns in children with more RTIs were characterized by enrichment of *Neisseria* spp. and (facultative) anaearobic, mainly oral species, including *Prevotella* spp., which in turn were linked to formula feeding. Similar findings have been reported previously (10, 30), and imply a loss of topography within the upper respiratory tract, suggesting that the host or the local ecosystem is unable to restrain oral microbiota within

their niche early in life. As presence of these bacteria is linked to RTI susceptibility, further studies on their role in respiratory health is warranted.

In literature, conflicting results have been reported regarding the role of *Moraxella* spp. in the pathogenesis of RTIs. Some studies found that *Moraxella* spp. colonization was associated with respiratory infections including pneumonia and bronchiolitis (11), while others reported that the *Moraxella*-dominated profile was associated with bacterial community stability (10, 20) and fewer RTI episodes (10). Although in our study, development from a *Staphylococcus*- into a *Corynebacterium/Dolosigranulum*-, towards a *Moraxella*-dominated profile eventually occurs in the great majority of children, we here show that especially lack of *Corynebacterium/Dolosigranulum* spp. establishment coincides with a premature transition from *Staphylococcus*- towards a *Moraxella*-dominated profile, which is associated with influx of oral bacterial species and an increased risk of RTIs (20). In line, several studies in mice have demonstrated that the neonatal immune system requires cues from the respiratory microbiota for its development within a specific time frame (12, 13). Indeed, premature *Moraxella* spp. colonization is shown to induce a mixed pro-inflammatory immune response (31), although data on the effects of *Moraxella* spp. colonization at later age are lacking. In addition, it deserves further study whether the required microbial triggers might be species and/or strain specific.

In our prospective, birth cohort study we collected frequent nasopharyngeal samples of a large number of healthy children at regular intervals over the first year of life as well as during RTIs, allowing us to study the microbial development during health, preceding and during RTI episodes. More importantly, it allowed us to explore microbiota dynamics and drivers of susceptibility to RTIs. Strengths of our study include the frequency of sampling and the consistency in data and sample collection by trained doctors and research nurses. We made a

rigorous effort to minimize the potential effect of environmental contamination on low-density nasopharyngeal samples collected from children at very early age. Last, we used non-parametric, machine-learning techniques combined with (multivariable) spline-based mixed models to explore specific age-dependent patterns in microbial succession.

Our study also has limitations. First, parents were asked to contact the research team in case of a RTI. Therefore, likely not all RTI episodes may have been captured for in depth analyses. Exhaustive efforts were however made to obtain detailed information on all experienced RTIs when questionnaires were filled out during regular home visits to minimize reporting bias in our multivariable analyses (Bosch *et al*, unpublished data). Second, despite frequent sampling, our samples capture snapshots of a highly dynamic and developing microbiome, therefore we can only make assumptions about the dynamics in between sampling moments. Third, although we observed that microbiota changes seem to forego RTIs and are associated with RTI susceptibility, our study design precludes any definite statements on causality.

We here provide evidence that accelerated microbiota maturation is associated with microbiota instability and number of RTIs over the first year of life. These changed dynamics could be observed as early as within the first month of age, i.e. prior to the first RTI experiences. We also were able to link the impact of known important drivers such birth mode, feeding type, the presence of siblings, early day-care attendance, and recent use of antimicrobial therapy, via altered microbiota development to susceptibility to RTIs. The potential implications of these findings for our understanding of pathogenesis of disease, as well as diagnostic and preventive strategies, deserves further investigation.

Acknowledgments

We gratefully acknowledge the department of Obstetrics and Gynecology of the Spaarne Gasthuis and participating midwifery clinics for recruiting participants for this study; the research team of the Spaarne Gasthuis Academy for their execution of and dedication to the study; the laboratory staff of the University Medical Center Utrecht and TNO for their lab work and the cooperating institutes for their commitment to the project. Most of all, we are indebted to all the participating children and their families.

Competing interests

No conflict of interest related to the present study. EAMS declares to have received unrestricted research support from Pfizer, grant support for vaccine studies from Pfizer and GSK and fees paid to the institution for advisory boards or participation in independent data monitoring committees for Pfizer and GSK. No other authors reported financial disclosures. Funding sources had no role in the study design, in the collection, analysis and interpretation of data, in writing the report, and the decision to submit the paper for publication. The corresponding author had full access to all the data in the study and had final responsibility for the decision to submit for publication.

References

1. Liu L, Oza S, Hogan D, Chu Y, Perin J, Zhu J, Lawn JE, Cousens S, Mathers C, Black RE. Global, regional, and national causes of under-5 mortality in 2000-15: an updated systematic analysis with implications for the Sustainable Development Goals. *Lancet* 2016;388:3027–3035.
2. Global Burden of Disease Study 2013 Collaborators. Global, regional, and national incidence, prevalence, and years lived with disability for 301 acute and chronic diseases and injuries in 188 countries, 1990-2013: a systematic analysis for the Global Burden of Disease Study 2013. *Lancet* 2015;386:743–800.
3. Donnelly JP, Baddley JW, Wang HE. Antibiotic utilization for acute respiratory tract infections in U.S. emergency departments. *Antimicrob Agents Chemother* 2014;58:1451–1457.
4. Bosch AATM, Levin E, van Houten MA, Hasrat R, Kalkman G, Biesbroek G, de Steenhuijsen Piters WAA, de Groot P-KCM, Pernet P, Keijser BJF, Sanders EAM, Bogaert D. Development of Upper Respiratory Tract Microbiota in Infancy is Affected by Mode of Delivery. *EBioMedicine* 2016;9:336–345.
5. Chu DM, Ma J, Prince AL, Antony KM, Seferovic MD, Aagaard KM. Maturation of the infant microbiome community structure and function across multiple body sites and in relation to mode of delivery. *Nat Med* 2017;23:314–326.
6. Bokulich NA, Chung J, Battaglia T, Henderson N, Jay M, Li H, D Lieber A, Wu F, Perez-Perez GI, Chen Y, Schweizer W, Zheng X, Contreras M, Dominguez-Bello MG, Blaser MJ. Antibiotics, birth mode, and diet shape microbiome maturation during early life. *Sci Transl Med* 2016;8:343ra82–343ra82.
7. Bogaert D, Keijser B, Huse S, Rossen J, Veenhoven R, van Gils E, Bruin J, Montijn R, Bonten M, Sanders E. Variability and diversity of nasopharyngeal microbiota in children: a metagenomic analysis. *PLoS ONE* 2011;6:e17035.
8. Biesbroek G, Bosch AATM, Wang X, Keijser BJF, Veenhoven RH, Sanders EAM, Bogaert D. The Impact of Breastfeeding on Nasopharyngeal Microbial Communities in Infants. *Am J Respir Crit Care Med* 2014;190:298–308.
9. Blaser MJ. Antibiotic use and its consequences for the normal microbiome. *Science* 2016;352:544–545.
10. Biesbroek G, Tsivtsivadze E, Sanders EAM, Montijn R, Veenhoven RH, Keijser BJF, Bogaert D. Early respiratory microbiota composition determines bacterial succession patterns and respiratory health in children. *Am J Respir Crit Care Med* 2014;190:1283–1292.
11. Vissing NH, Chawes BLK, Bisgaard H. Increased risk of pneumonia and bronchiolitis after bacterial colonization of the airways as neonates. *Am J Respir Crit Care Med* 2013;188:1246–1252.
12. Gollwitzer ES, Saglani S, Trompette A, Yadava K, Sherburn R, McCoy KD, Nicod LP, Lloyd CM, Marsland BJ. Lung microbiota promotes tolerance to allergens in neonates via PD-L1. *Nat Med* 2014;20:642–647.
13. Olszak T, An D, Zeissig S, Vera MP, Richter J, Franke A, Glickman JN, Siebert R, Baron RM, Kasper DL, Blumberg RS. Microbial exposure during early life has persistent effects on natural killer T cell function. *Science* 2012;336:489–493.
14. Hooper LV, Littman DR, Macpherson AJ. Interactions between the microbiota and the immune system. *Science* 2012;336:1268–1273.
15. Kamada N, Chen GY, Inohara N, Núñez G. Control of pathogens and pathobionts by the gut microbiota. *Nat Immunol* 2013;14:685–690.
16. Man WH, de Steenhuijsen Piters WAA, Bogaert D. The microbiota of the respiratory tract: gatekeeper to respiratory health. *Nat Rev Microbiol* 2017;8:51.

17. Pettigrew MM, Laufer AS, Gent JF, Kong Y, Fennie KP, Metlay JP. Upper respiratory tract microbial communities, acute otitis media pathogens, and antibiotic use in healthy and sick children. *Appl Environ Microbiol* 2012;78:6262–6270.
18. Hilty M, Qi W, Brugger SD, Frei L, Agyeman P, Frey PM, Aebi S, Muhlemann K. Nasopharyngeal microbiota in infants with acute otitis media. *J Infect Dis* 2012;205:1048–1055.
19. de Steenhuijsen Piters WAA, Heinonen S, Hasrat R, Bunsow E, Smith B, Suarez-Arrabal M-C, Chaussabel D, Cohen DM, Sanders EAM, Ramilo O, Bogaert D, Mejias A. Nasopharyngeal Microbiota, Host Transcriptome, and Disease Severity in Children with Respiratory Syncytial Virus Infection. *Am J Respir Crit Care Med* 2016;194:1104–1115.
20. Teo SM, Mok D, Pham K, Kusel M, Serralha M, Troy N, Holt BJ, Hales BJ, Walker ML, Hollams E, Bochkov YA, Grindle K, Johnston SL, Gern JE, Sly PD, Holt PG, Holt KE, Inouye M. The infant nasopharyngeal microbiome impacts severity of lower respiratory infection and risk of asthma development. *Cell Host and Microbe* 2015;17:704–715.
21. de Steenhuijsen Piters WAA, Sanders EAM, Bogaert D. The role of the local microbial ecosystem in respiratory health and disease. *Philosophical Transactions of the Royal Society B: Biological Sciences* 2015;370:20140294.
22. O'Brien KL, Nohynek H, World Health Organization Pneumococcal Vaccine Trials Carraige Working Group. Report from a WHO working group: standard method for detecting upper respiratory carriage of Streptococcus pneumoniae. *Pediatr Infect Dis J* 2003;22:133–140.
23. Wyllie AL, Chu MLJN, Schellens MHB, van Engelsdorp Gastelaars J, Jansen MD, van der Ende A, Bogaert D, Sanders EAM, Trzciński K. Streptococcus pneumoniae in Saliva of Dutch Primary School Children. *PLoS ONE* 2014;9:e102045.
24. Subramanian S, Huq S, Yatsunenko T, Haque R, Mahfuz M, Alam MA, Benezra A, DeStefano J, Meier MF, Muegge BD, Barratt MJ, VanArendonk LG, Zhang Q, Province MA, Petri WA, Ahmed T, Gordon JI. Persistent gut microbiota immaturity in malnourished Bangladeshi children. *Nature* 2014;510:417–421.
25. Dominguez-Bello MG, Costello EK, Contreras M, Magris M, Hidalgo G, Fierer N, Knight R. Delivery mode shapes the acquisition and structure of the initial microbiota across multiple body habitats in newborns. *Proc Natl Acad Sci USA* 2010;107:11971–11975.
26. Laufer AS, Metlay JP, Gent JF, Fennie KP, Kong Y, Pettigrew MM. Microbial communities of the upper respiratory tract and otitis media in children. *mBio* 2011;2:e00245–10.
27. Hunt KM, Foster JA, Forney LJ, Schütte UM, Beck DL, Abdo Z, Fox LK, Williams JE, McGuire MK, McGuire MA. Characterization of the diversity and temporal stability of bacterial communities in human milk. *PLoS ONE* 2011;6:e21313.
28. Bomar L, Brugger SD, Yost BH, Davies SS, Lemon KP. Corynebacterium accolens Releases Antipneumococcal Free Fatty Acids from Human Nostril and Skin Surface Triacylglycerols. *mBio* 2016;7:.
29. Prevaes SMPJ, de Winter-de Groot KM, Janssens HM, de Steenhuijsen Piters WAA, Tramper-Stranders GA, Wyllie AL, Hasrat R, Tiddens HA, van Westreenen M, van der Ent CK, Sanders EAM, Bogaert D. Development of the Nasopharyngeal Microbiota in Infants with Cystic Fibrosis. *Am J Respir Crit Care Med* 2016;193:504–515.
30. Holgerson PL, Vestman NR, Claesson R, Ohman C, Domellöf M, Tanner ACR, Hernell O, Johansson I. Oral microbial profile discriminates breast-fed from formula-fed infants. *J Pediatr Gastroenterol Nutr* 2013;56:127–136.

31. Følsgaard NV, Schjørring S, Chawes BL, Rasmussen MA, Krogfelt KA, Brix S, Bisgaard H. Pathogenic bacteria colonizing the airways in asymptomatic neonates stimulates topical inflammatory mediator release. *Am J Respir Crit Care Med* 2013;187:589–595.
32. Clarke KR. Non-parametric multivariate analyses of changes in community structure. *Australian journal of ecology* 1993;doi:10.1111/j.1442-9993.1993.tb00438.x/full.

Figure legends

Figure 1 – Microbiota development over the first year of life.

(A) Relative abundance of the 15 highest ranking OTUs over the first year of life (age in days) and during of RTIs. OTUs are colour coded as indicated in the figure legend, which was based on their phylum level taxonomic annotation: red, Firmicutes; yellow, Actinobacteria; blue, Proteobacteria and green, Bacteroidetes. We observed a high abundance of Firmicutes (*Staphylococus (3)* and *Dolosigranulum (4)*) and Actinobacteria (*Corynebacterium* spp.) early in life, which was gradually replaced by Proteobacteria (*Moraxella (1)*, *Moraxella (7)*, *Haemophilus (6)* and *Neisseria* spp.). OTUs that were not among the 15 highest ranking were collapsed and referred to as 'Residuals', stratified by phylum for the five most abundant phyla.

(B) Relative abundance of the 15 highest ranking OTUs over the first two months of life. Visualisation of microbiota profiles per time point allows for a more detailed assessment of microbial dynamics at early time points. Over the first week of life, a relatively high abundance of *Streptococcus (5)*, *Janthinobacterium (13)* and *Neisseria* spp. and *Rothia (12)* was observed, apart from other OTUs belonging mainly to the Firmicutes, Proteobacteria and Actinobacteria phyla (See Figure E5). d = day; w = week; m = month.

Figure 2 – Non-metric multidimensional scaling (nMDS) plot visualizing the microbiota succession patterns in the first year of life.

Each point represents the microbial community composition of one sample. Samples taken during health (n=1,065) are coloured based on the age at which they were taken (colours ranging from yellow [day 0] to dark green [year 1]). In addition, samples taken during RTI are depicted (n=56; dark red). The standard deviation of data points within time point/RTI strata is shown by ellipses. The 15 highest ranked OTUs were simultaneously visualized (triangles).

The size of the triangles is relative to the mean relative abundance of the OTU it represents. The stress value indicates how well the high-dimensional data are captured in the two-dimensional space; a value of ~0.2 indicates that the representation of some points is potentially misleading and that a representation in a higher dimensional space might be more appropriate (see Figure E4 for detailed assessment) (32). d = day; w = week; m = month; RTI = respiratory tract infection.

Figure 3 – Absolute bacterial density over the first year of life.

Boxplots showing the absolute bacterial density (in pg/µL 16S-rRNA-gene) in blanks (n=55; blue), in samples taken during health at various time points (n=1,065; colours ranging from yellow [day 0] to dark green [year 1]) and during RTI (n=56; red). Bacterial density is particularly low at days 0 and 1, then gradually increases until the age of ~1 month, after which it remained largely stable. Box plots represent the 25^{th} and 75^{th} percentiles (lower and upper boundaries boxes, respectively), the median (middle horizontal line), and measurements that fall within 1.5 times the interquartile range (IQR; distance between 25^{th} and 75^{th} percentiles; whiskers) or outside 1.5 times the IQR (points). Q-values were derived from a linear mixed model with $\log_{10}$-transformed bacterial density as outcome variable, time point as fixed effect and subject as a random effect. Only samples taken at regular intervals were considered and each consecutive time point was compared to the previous time point using the *multcomp* package. ***, q-value <0.001; **, 0.001 ≤q-value <0.01. d = day; w = week; m = month; RTI = respiratory tract infection.

Figure 4 – Microbiota maturation and age-discriminatory taxa stratified by RTI susceptibility.

(A) Microbiota age estimates plotted against chronological age stratified by number of RTIs experienced during the first year of life. The curves represent smooth spline fits for each cohort.

P-values are based on a linear mixed model, including age (spline) and number of RTIs (i.e. 0-2, 3-4 or 5-7 RTIs) as fixed effects and subject as random effect.

(B) Heatmap of the mean relative abundance of the 22 age-discriminatory OTUs against moment of sampling in each cohort. OTUs are ordered vertically based on average linkage hierarchical clustering using the Euclidean distance matrix. Colours correspond with row wise normalized relative abundances (i.e. red indicates the maximum relative abundance of that OTU over all cohorts, black indicates the minimum relative abundance). OTU-names are bold and coloured green if they were significantly enriched in the reference group (0-2 RTIs) compared to children with >2 RTIs. Red was used to denote the OTUs that were observed in higher abundance in children with >2 RTIs (based on SS-ANOVA q-values; see Table 4A). d = day; w = week; m = month; RTI = respiratory tract infection.

(C) Relative microbiota age (RMA) before (light green shades), during (red) and after RTI (dark green). The relative microbiota age two time points before RTI ('-2'; n=51; on average -104 days to RTI), one time point before RTI ('-1'; n=47; -50 days to RTI), at RTI ('RTI'; n=56; mean age at sampling of 216 days) and after RTI ('+1'; n=41; +57 days after RTI) is depicted in boxplots (see legend Figure 2). RMA already increased at time points preceding a factual RTI (median RMA +7.3 days at T = -2, +37.1 days at T = -1, and +67.8 days at RTI). P-values are based on a linear mixed model including timing of sampling (i.e. '-2', '-1', 'RTI' or '+1') and age (continuous) as fixed effects and subject as random effect. The contrasts '-2' vs '-1', '-1 vs 'RTI' and 'RTI' vs '+1' were tested (*multcomp* package). **, 0.001 ≤q-value <0.01; *, 0.01 ≤q-value <0.05.

Figure 5 – Microbiota stability over time stratified by RTI susceptibility.

Bray-Curtis dissimilarities were calculated within each subject between each pair of

685 consecutive time points. The bacterial community stability was significantly lower in children
686 with 3-4 (p=0.005) or 5-7 RTIs (p=0.02) compared to the reference group of children
687 experiencing 0-2 RTIs within the first year of life. P-values are based on a linear mixed model,
688 including age (spline) and number of RTIs as fixed effects and subject as random effect. The
689 shaded area around each smoothing spline represents the 95% confidence interval.

690

Legends Online Supplement

Methods – Online supplement methods.

Figure E1 – Flow chart study.

Flow chart showing the number of initially enrolled women and the reasons for exclusion of participants.

Figure E2 – Distribution of respiratory tract infections within the cohort.

Histogram of the number of RTIs versus their frequency. '*N*' denotes the number of individuals, '*n*' gives the number of samples. The cohort was divided in RTI groups based on the distribution of RTIs; each sub cohort corresponds with a tertile.

Figure E3 – OTU selection procedure.

(A) Plot showing the 10-fold cross-validation error (mean ±standard deviation) as a function of the number of OTUs used to regress against chronological age in the reference cohort (children with 0-2 RTIs). An optimal trade-off between the mean squared error (MSE; i.e. cross-validation error) and number of OTUs in the model was observed at 22 OTUs.

(B) Age-discriminatory OTUs ranked in descending order based on their importance to the accuracy of the model. OTU importance was estimated by calculating the increase in mean-squared error (MSE) of the microbiota age prediction after randomly permuting the relative abundance values of each given OTU (mean ±standard deviation, 100 replicates).

Figure E4 – nMDS diagnostic plots and three-dimensional nMDS.

(A) Scree plot to depict the relationship between the number of (nMDS)-dimensions and stress. Naturally, the stress will reduce by increasing the number of dimensions, however only a maximum number of three dimensions can reasonably be interpreted. Using three dimensions the stress-value drops well below 0.2 (32), suggesting that a decent ordination of the data is possible in this number of dimensions.

(B) Three-dimensional nMDS plot. The main data structure visualized using the two-dimensional plot appears to be preserved when plotting the same data in three dimensions.

Figure E5 – Relative abundance of early colonizing bacteria.

Bar plots visualizing the relative abundance (mean ±standard error of the mean) of the 10 highest ranking OTUs at each (early) time point (only considering day 0 and 1 and week 1 and 2). For each OTU, we calculated the significance of change in relative abundance for each pair of consecutive time points (i.e. day 0 vs day 1, day 1 vs week 1 and week 1 vs week 2) using mixed linear models including subject as random effect. Significant differences between contrasts were determined using the *multcomp*-package. A Benjamini-Hochberg procedure was used to correct for multiple comparisons (simultaneously considering all OTUs/contrasts). ***, q-value <0.001; **, 0.001 ≤q-value <0.01; *, 0.01 ≤q-value <0.05.

Figure E6 – Individual microbial developmental trajectories in time.

Using average linkage hierarchical clustering based on the Bray-Curtis dissimilarity matrix samples were binned into 8 clusters consisting of ≥10 samples. These clusters were enriched for *Moraxella (1)* (MOR1) *Corynebacterium (2)* and *Dolosigranulum (4)* (CDG), *Staphylococcus (3)* (STA) and *Streptococcus (5)* (STR), *Moraxella (7)* (MOR7), *Haemophilus (6)* (HAE), *Corynebacterium (8)* (COR8) and *Neisseria* spp. (NEI). The number of individuals in each cluster at each time point was visualised in alluvial diagrams, which were stratified by

the number of RTIs experienced over the first year of life (i.e. **(A)** 0-2 RTIs, **(B)** 3-4 RTIs and **(C)** 5-7 RTIs). The height of the figures corresponds with the total number of samples within that group. In addition, the height of the nodes and the thickness of the lines connecting the nodes is proportional to the number of samples. We observed that the CDG-cluster is underrepresented in children who experienced 5-7 RTIs over time. Instead, the early-life STA-cluster rapidly transitions into the MOR1-cluster, which is associated with older ages.

Figure E7 – Relative abundance of age-discriminatory taxa at each time point. The line plots indicate the microbiota development for each age-discriminatory taxum. Dots represent mean relative abundance at a given time point within the stratum and whiskers depict the standard error of the mean. See Table E4 for statistical assessment. d = day; w = week; m = month.

Figure E8 – Relative microbiota age stratified by time point and RTI cohort.

Boxplots (see legend Figure 3) depicting relative microbiota age (RMA) for each cohort. The RMA was significantly higher in children who experienced 5-7 RTIs compared to the reference group, after adjusting for either age or sampling moment (both p=0.007).

Figure E9 – Relative abundance of age-discriminatory taxa before (light green shades), during (red) and after RTI (dark green; see also legend figure 4C). Relative abundances were depicted using boxplots (see legend Figure 3). We tested the statistical significance of differences in microbial abundance between sampling moments using a linear mixed model including timing of sampling (i.e. '-2', '-1', 'RTI' or '+1') and age (continuous) as fixed effects and subject as random effect. The contrasts '-2' vs '-1', '-1 vs 'RTI' and 'RTI' vs '+1' were tested (*multcomp* package). Although we did observe changes in abundance of individual OTUs that appeared to be related to changes in RMA, these changes were not statistically significant (after adjusting for multiple testing).

Figure E10 – α-diversity measures stratified by RTI susceptibility.

We tested the number of observed species, Simpson and Shannon diversity indices. No significant differences between RTI groups were observed. Points represent mean values and whiskers depict the standard error of the mean. P-values were derived from mixed linear models with subject as random effect and adjusted for age (spline); p>0.05). d = day; w = week; m = month.

Figure E11 – Relative abundance of the 15 highest ranking OTUs during the first year of life stratified by birth mode and feeding type - flow diagram.

See legend Figure 1A. We observed an increased relative abundance of *Corynebacterium (2)* and *Dolosigranulum (4)* until the age of five months and late *Moraxella* spp. enrichment in children vaginally delivered and/or breastfed. Birth by caesarean section was associated with early *Staphylococcus (3)* predominance. Feeding type was studied as a categorical variable indicating whether children were exclusively breastfed (BF) up to the age of three months (3m). See Table E6 and E7 for statistical assessment.

Figure E12 – Relative abundance of the 15 highest ranking OTUs during the first year of life stratified by birth mode and feeding type - line plots.

(A) Line plots indicating the microbiota succession patterns of abundant taxa, stratified by birth mode (caesarean section vs vaginal). Points represent means and whiskers represent standard errors of the mean. See Table E6 for statistical assessment. d = day; w = week; m = month; RTI = respiratory tract infection.

(B) Line plots indicating the microbiota succession patterns of abundant taxa, stratified by feeding type (exclusive breastfeeding up to the age of three months yes/no). Points represent

means and whiskers represent standard errors of the mean. See Table E10 for statistical assessment. d = day; w = week; m = month; RTI = respiratory tract infection.

Figure 1

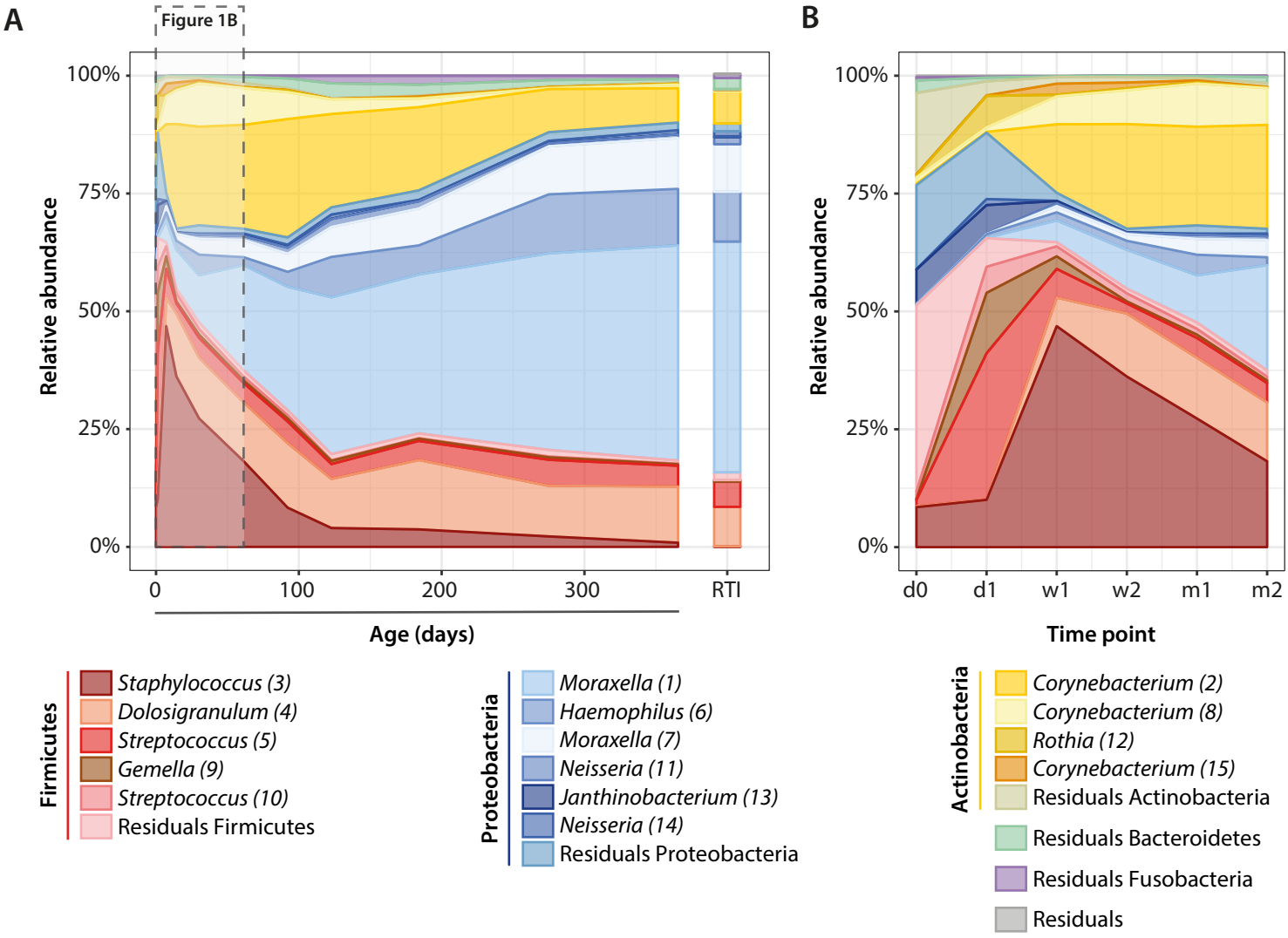
A
Figure 1B
100%
75%
50%
25%
0%
Relative abundance
0
100
200
300
RTI
Age (days)
B
100%
75%
50%
25%
0%
Relative abundance
d0
d1
w1
w2
m1
m2
Time point
Firmicutes
Staphylococcus (3)
Dolosigranulum (4)
Streptococcus (5)
Gemella (9)
Streptococcus (10)
Residuals Firmicutes
Proteobacteria
Moraxella (1)
Haemophilus (6)
Moraxella (7)
Neisseria (11)
Janthinobacterium (13)
Neisseria (14)
Residuals Proteobacteria
Actinobacteria
Corynebacterium (2)
Corynebacterium (8)
Rothia (12)
Corynebacterium (15)
Residuals Actinobacteria
Residuals Bacteroidetes
Residuals Fusobacteria
Residuals

Figure 2

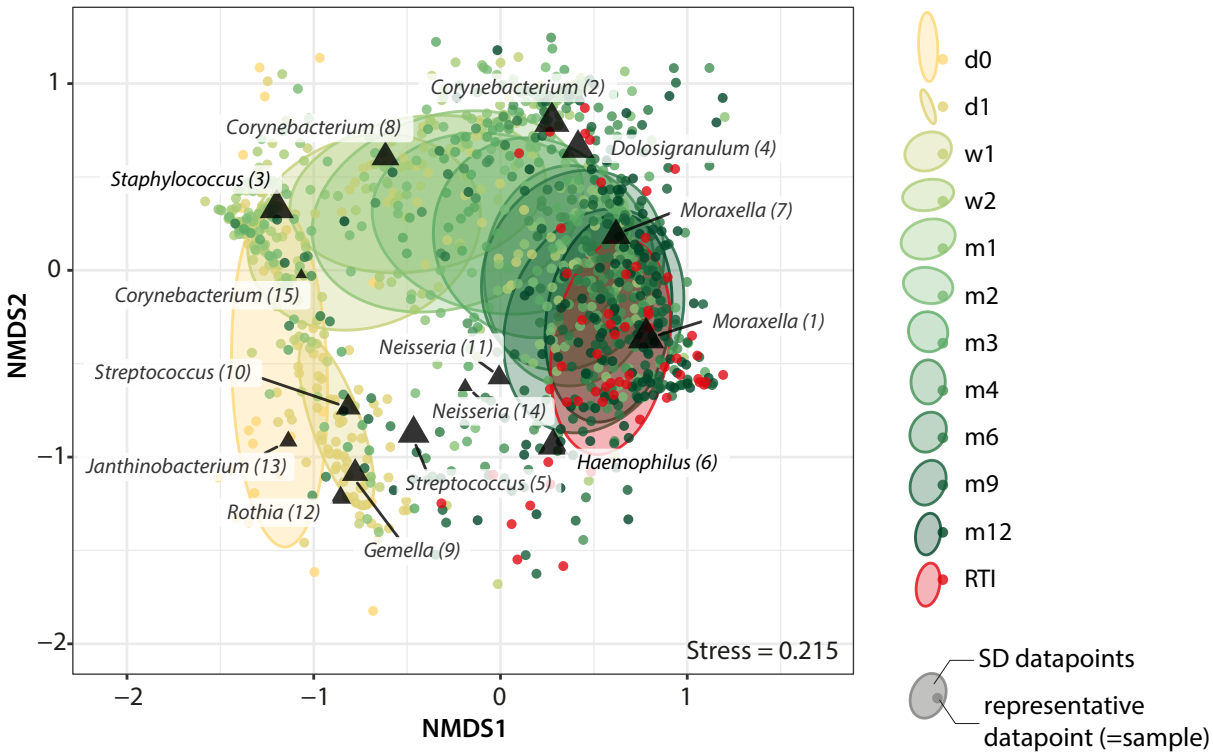
Corynebacterium (2)
Corynebacterium (8)
Dolosigranulum (4)
Staphylococcus (3)
Moraxella (7)
Corynebacterium (15)
Moraxella (1)
Neisseria (11)
Streptococcus (10)
Neisseria (14)
Haemophilus (6)
Janthinobacterium (13)
Streptococcus (5)
Rothia (12)
Gemella (9)
Stress = 0.215
NMDS1
NMDS2
1
0
−1
−2
−2
−1
0
1
d0
d1
w1
w2
m1
m2
m3
m4
m6
m9
m12
RTI
SD datapoints
representative datapoint (=sample)

Figure 3

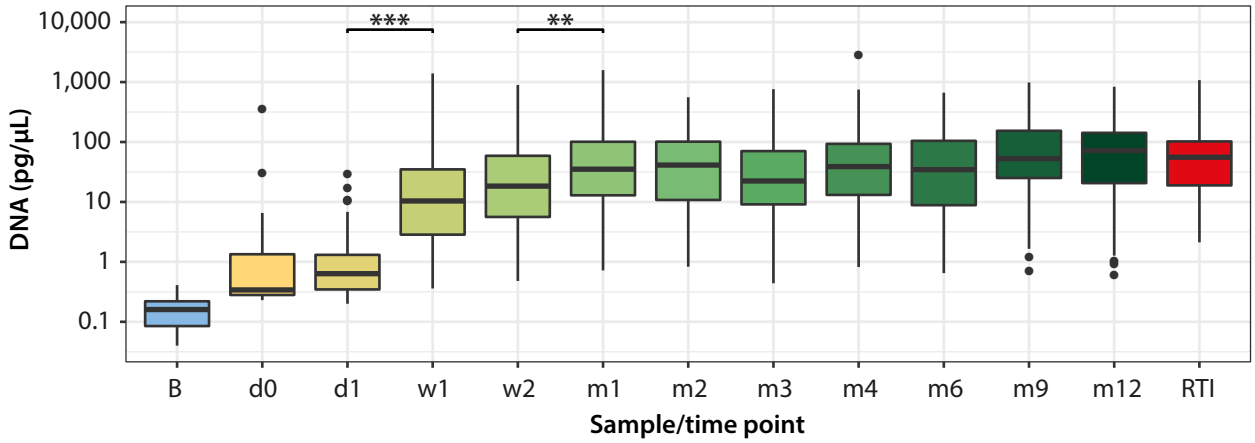
10,000
1,000
100
10
1
0.1
DNA (pg/µL)
***
**
B
d0
d1
w1
w2
m1
m2
m3
m4
m6
m9
m12
RTI
Sample/time point

Figure 4

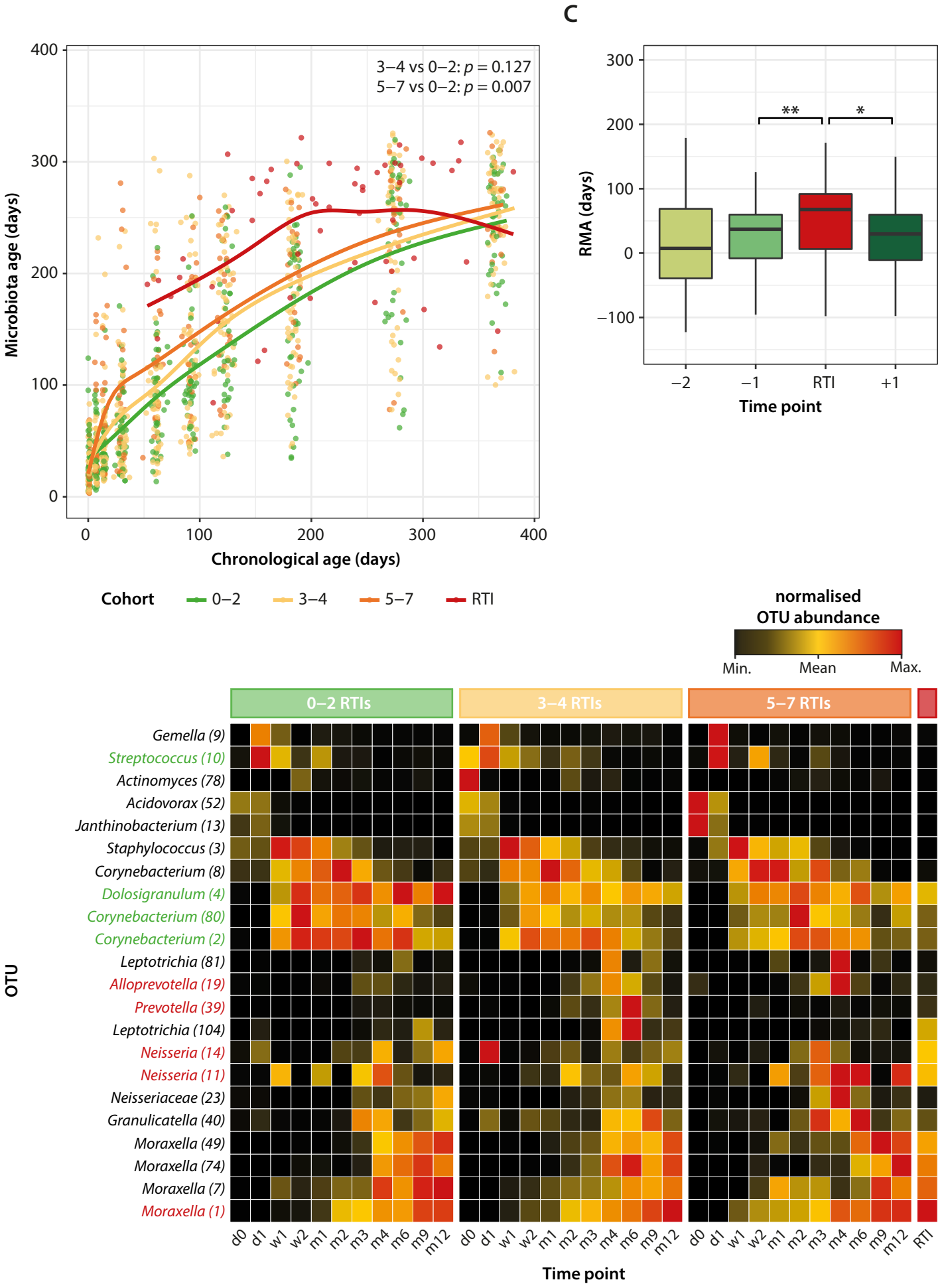
A
3–4 vs 0–2: p = 0.127
5–7 vs 0–2: p = 0.007
Microbiota age (days)
Chronological age (days)
Cohort
0–2
3–4
5–7
RTI
C
RMA (days)
Time point
**
*
−2
−1
RTI
+1
B
normalised
OTU abundance
Min.
Mean
Max.
0–2 RTIs
3–4 RTIs
5–7 RTIs
OTU
Gemella (9)
Streptococcus (10)
Actinomyces (78)
Acidovorax (52)
Janthinobacterium (13)
Staphylococcus (3)
Corynebacterium (8)
Dolosigranulum (4)
Corynebacterium (80)
Corynebacterium (2)
Leptotrichia (81)
Alloprevotella (19)
Prevotella (39)
Leptotrichia (104)
Neisseria (14)
Neisseria (11)
Neisseriaceae (23)
Granulicatella (40)
Moraxella (49)
Moraxella (74)
Moraxella (7)
Moraxella (1)
d0 d1 w1 w2 m1 m2 m3 m4 m6 m9 m12
RTI
Time point

Figure 5

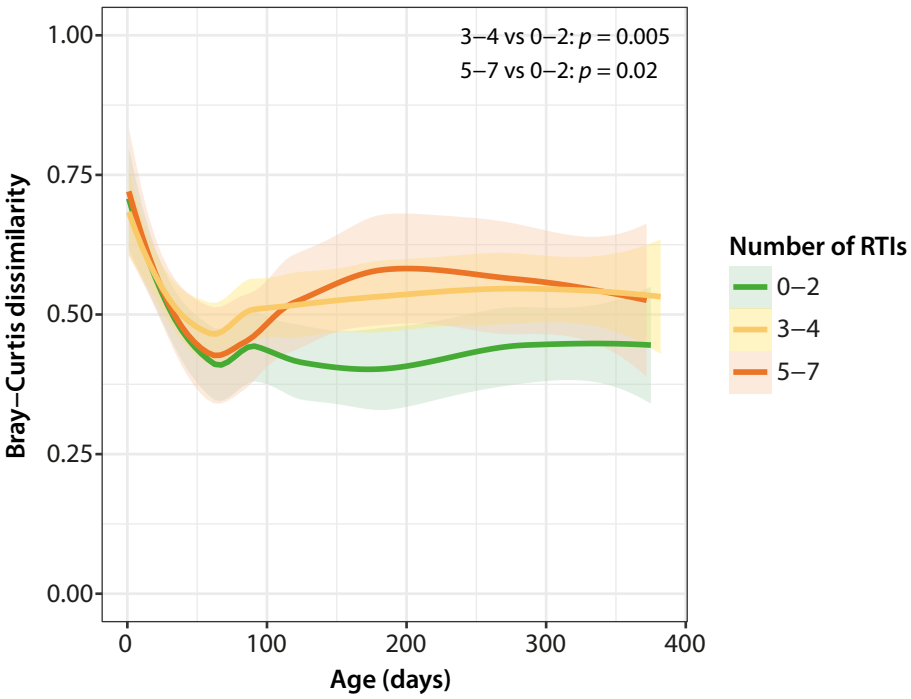
3–4 vs 0–2: p = 0.005
5–7 vs 0–2: p = 0.02
Bray–Curtis dissimilarity
1.00
0.75
0.50
0.25
0.00
0
100
200
300
400
Age (days)
Number of RTIs
0–2
3–4
5–7

ONLINE SUPPLEMENT

Title: Maturation of the infant respiratory microbiota, environmental drivers and health consequences: a prospective cohort study

Authors: Astrid A.T.M. Bosch[†], Wouter A.A. de Steenhuijsen Piters[†], Marlies A. van Houten, Mei Ling J.N. Chu, Giske Biesbroek, Jolanda Kool, Paula Pernet, Pieter-Kees C.M. de Groot, Marinus J.C. Eijkemans, Bart J.F. Keijser, Elisabeth A.M. Sanders and Debby Bogaert*

[†] These authors contributed equally to this work

* Corresponding author. Email: D.Bogaert@ed.ac.uk.

This file includes:

(Online supplement) Methods

Other supplementary materials for this manuscript include the following:

Figures E1-E12, as a separate pdf-file.

Tables E1-E7, including captions, as a separate excel spreadsheet.

Methods

Study population

Nasopharyngeal swabs were collected from healthy children who participated in an ongoing prospective birth cohort study. The primary aim of this population-based study is to investigate the development and dynamics of the microbiota in infants during health and disease, with special interest in the impact of mode of delivery on microbial succession. Since approximately 15% of the Dutch children are born by caesarian section (E1), the cohort is enriched by caesarian section deliveries with the aim to obtain a ~50/50 distribution between caesarian section born children and vaginally delivered children. The study is conducted in the Netherlands, a small country (approximately 17 million inhabitants) in North-Europe with high socio-economic standards and a moderate sea climate characterized by cool summers and mild winters.

The trials' methods have been described elsewhere (E2). In short, healthy, term born newborns (gestational age >37 weeks) were enrolled in the study directly after birth. Exclusion criteria at baseline were major congenital anomalies, severe maternal or neonatal complications during birth, language barrier, intention to move outside the research area, or parents under the age of 18 years. Written informed consent was obtained from both parents before birth of the child. Participants did not receive any financial compensation. An acknowledged national Ethics Committee in the Netherlands (METC Noord-Holland, committee on research involving human subjects) approved the study (M012-015, NH012.394, NTR3986). The study was conducted in accordance with the European Statements for Good Clinical Practice. We estimated 10-20% loss to follow-up, therefore we had ethical approval to replace participants in case they dropped out of the study before six months of follow-up. Eventually we had complete datasets up to one

year of age of 116 participants. These infants were born between December 19th, 2012 and November 2st, 2014.

Of these 116 children, we had at least eight samples of good quality available for 112 children after laboratory work-up (Figure E1).

Our study was powered to detect differences in microbial communities between vaginally born children and children born by caesarian-section, which was the primary aim of the cohort study. We performed power calculations aiming to be able to detect at least two-fold differences in at least the top 25 most common bacteria after correction for multiple testing. Given the variability and spread in abundance of OTUs we calculated that 40 children per group would give us sufficient power (>80%) to address our primary research question. Because the inclusion rate of caesarian-born children was lower than expected, we were allowed to extend the enrollment period, resulting in a much larger sample size (N=128) than initially expected, enabling us to thoroughly investigate secondary outcomes, such as the association between microbiota differences and the number of RTIs, again providing us with sufficient power to analyze group sizes of approximately 40 children per group.

Data collection

Home visits were conducted directly after birth, 24 hours after birth, at seven days, 14 days, and one, two, three, four, six, nine, and 12 of months of age. Postpartum visits were all performed within two hours from birth and all day one samples were obtained within 24-36 hours after delivery. For logistic reasons (sampling preferably during office hours and considering parental vacations), we allowed some flexibility for the remaining sample moments: all week one samples were obtained within 5-9 days (mean 7); all week two samples between 12-17 days (mean 14); month one samples between 23-27 days (mean 30), months two

samples between 49-73 days (mean 61), months three samples between 83-11 days (mean 92), months four samples between 112-133 days (mean 123), months six between 177-197 days (mean 184), months nine samples between 260-288 (mean 275), months 12 samples between 358-382 (mean 366) days postpartum, resulting in no overlap between sample moments (see Figure 4A).

Each home visit, nasopharyngeal samples were obtained by trained doctors and research nurses in a semi-sterile setting as previously described (E2). In short, deep nasopharyngeal swabs were collected trans nasally using a flexible, sterile swab (Copan eSwab, 484CE). Directly after sampling, the swabs were snap-frozen and stored in a sterile, filtered solution (10% Glycerol (VWR international BV 1.04093.1000) in 0.1% DEPC water (SERVA Electrophoresis, 39798.03). The swabs were transported on dry ice and stored at -80°C until further analyses. In addition, the research team completed an extensive survey on the health status of the child and environmental factors, including breastfeeding, crowding conditions, and medication use.

Next to these regular and frequent visits, parents were asked to contact the study team in case of an active respiratory tract infections, defined as fever ≥38°C (per rectal measurement) for >6 hours combined with general unwell feeling and presence of RTI symptoms, including earache, cough, hoarseness, wheeze, dyspnoea and/or runny nose. During an extra home visit (RTI visit within 48 hours after start of the fever), we collected additional nasopharyngeal samples using the same procedure as described above and obtained information about the duration of the fever, RTI symptoms, and antibiotic use. In addition, the research team called parents two to four weeks after the RTI visit to complete the questionnaire. Since 15 of the children had respiratory symptoms with fever during one of the regular visits, these were also considered as a RTI episode in the analyses.

Bacterial DNA isolation and quantification

Bacterial DNA from 200 μl sample was isolated by bead-beating in phenol (E3) and quantified using a qPCR with primers directed at the 16S-rRNA gene (E4, 5). DNA was then eluted in two aliquots of 25 µl elution buffer and stored at -20°C until further analyses.

16S-rRNA gene amplicon sequencing

PCR amplicon libraries were generated by amplification of the 16S ribosomal RNA gene using barcoded primers directed at the V4 hypervariable region, as previously described (E2). Primer pair 533F/806R was used for amplification. Amplicon pools from samples and controls were sequenced in eight runs using an Illuminia MiSeq instrument, resulting in paired-end 200 or 250 nucleotide reads. We first trimmed all reads to a length of 200 nucleotides (Fastx toolkit, version 0.0.13) and then applied an adaptive, window-based trimming algorithm (Sickle, version 1.33) (E6) using a quality threshold of Q30 and a length threshold of 150 nucleotides to filter out low quality reads/nucleotides. We aimed to further reduce the number of sequence errors in the reads by applying an error correction algorithm (BayesHammer, SPAdes genome assembler toolkit, version 3.5.0) (E7). After quality filtering and error correction, reads were assembled into contigs (PANDAseq, version 2.9) (E8, 9) and demultiplexed (Qiime version 1.9.1; split_libraries.py) (E10). We removed singleton sequences (1.4%) and identified chimeras using both *de novo* and reference chimera identification (UCHIME; 3.2%). After removal of chimeric sequences, VSEARCH abundance-based greedy clustering was used to pick OTUs at a 97% identity threshold (E11). OTUs were then annotated by the Naïve Bayesian RDP classifier (version 2.2) (E12) with a classification confidence of 50% (default) (E13) and annotations were based on the 97% identity SILVA 119 release reference database (E14). The SILVA-annotations for the most abundant/age-discriminatory taxa were verified using

BLASTN (E15) (Table E1). In the main text we further refer to OTUs using maximum genus level annotations, combined with a rank number based on the abundance of each given OTU.

Data normalisation and filtering

We generated an abundance-filtered dataset by including only those OTUs that were present at or above a confident level of detection (0.1% relative abundance) in at least two samples, retaining 576 OTUs (0.3% of reads excluded) (E16). We generated a rarefied OTU-table at a sequence depth of 3,500 reads, calculated the relative abundance of OTUs and used this table as input for downstream analyses, including visualisations, random forest modelling and stability analyses. α-diversity measures were calculated for 100 rarefactions at a sequencing depth of 3500 reads and averaged. Raw read counts were normalised intrinsically using cumulative sum scaling (CSS) if modelling was performed using the *metagenomeSeq* package and the *fitTimeSeries* function (E17). Using this function, the temporal associations between each of the 22 age-discriminatory taxa and risk of RTIs were assessed; only significant results were reported. For the analyses on the temporal effects of birth mode and feeding type, OTUs with >10 sequences in ≥50 samples were included. Similarly, for analyses based on Multivariate Association with Linear Models (MaAsLin), we selected OTUs from the rarefied OTU-table with a relative abundance of >0.1% in ≥50 samples. Next, de OTU-table was expanded by calculating the cumulative relative abundance of the selected OTUs at all taxonomic levels (i.e. ranging from species/OTU-level to kingdom level). β-diversity was assed using the Bray-Curtis dissimilarity metric.

Quality control of 16S-rRNA gene amplicon sequencing

URT samples, especially in very young children, are typically low in bacterial density (E18), and therefore measures to control for potential contamination with environmental of DNA are

of vital importance. Since we were particularly interested in the initial colonization patterns of the children in our cohort, we set out to discern samples with a high likelihood of environmental contamination, from those samples that did not resemble negative DNA blanks through an unsupervised clustering approach. Both low DNA samples (0.2 pg/µl-0.5 pg/µl) and blanks (n=50; 30 excluded because of too low sequence depth) were rarefied to a depth of 2,000 reads and subjected to average linkage hierarchical clustering based on the Bray-Curtis dissimilarity (100 repeats). For each repeat, we used the maximum Silhouette index to determine the optimal number of clusters (up to 20 clusters tested). Samples that co-clustered with DNA blanks in >5% of the repeats were excluded from subsequent analyses, together with samples that were sequenced twice, samples with a density of <0.2 pg/µl or read counts <3,500 sequences, and samples of individuals that were lost to follow-up and/or had <8 samples available (in total 211 samples excluded), resulting in 1,121 samples from 112 individuals. Sequence data of part of the samples (≤6 months) of part of the children (743 samples, 101 individuals) were used for a previous study on the role of mode of delivery on early respiratory microbiota development (E2).

In addition, we included 14 mock communities, consisting of 12 bacterial species commonly observed in the upper respiratory tract (i.e. *Bacteroides fragilis*, *Haemophilus influenzae*, *Streptococcus pneumoniae*, *Streptococcus pyogenes*, *Klebsiella oxytoca*, *Klebsiella pneumoniae,* haemolytic *Streptococcus* group A*, Pseudomonias aeruginosa*, *Staphylococcus epidermidis*, *Staphylococcus aureus* and *Moraxella catarrhalis*). Equivalent amounts of DNA isolated from these species were combined and included as internal controls in the Illumina MiSeq runs.

Statistical analysis

All analyses were performed in the R version 3.3.0 within R studio version 0.99.902. All figures were created using the *ggplot2* R-package and edited using Illustrator CC. We corrected for multiple testing if applicable using the Benjamini-Hochberg procedure (resulting in corrected P-values or q-values; *p.adjust* function). 'Environmental factors' used in the descriptions of the various models below comprises birth mode, breast feeding until three months of age, day care attendance, presence of siblings under five years of age, antibiotic treatment in the previous four weeks and season of birth, if not specified otherwise.

Baseline tables

Baseline tables were created using the *tableone* package (E19). Continuous variables were tested for normality using a Shapiro-Wilk test. Variables with a non-normal distribution were characterised using a median and interquartile range and the statistical significance of differences between groups was calculated using a Mann-Whitney U or Kruskal-Wallis test. Normally distributed variables were summarised by a mean and standard deviation and differences were tested for significance using a Student's t-test/analysis of variance (ANOVA). For categorical variables, we used a Chi-square to test for statistically significant differences between groups. A Fisher's exact test was used for categorical variables if the expected cell count was less than five.

Non-metric multidimensional scaling and multivariate modelling

Microbial succession patterns were visualised using non-metric multidimensional scaling (nMDS; *metaMDS* function in the *vegan* package; trymax=1,000) (E20) based on the Bray-Curtis dissimilarity matrix. Ellipses were calculated using the *veganCovEllipse* function and represent the standard deviation of data points. Stress-values, which indicate how well the ordination captured the high-dimensional data (i.e. a measure of goodness-of-fit), were

reported. We tested whether a nMDS-visualisation in a higher dimensional space would decrease the stress of the ordination using a scree plot (1-6 dimensions tested). Based on our findings (balancing number of dimensions, reduction in stress-value and interpretability of the plot) we decided to provide a three-dimensional nMDS plot as a supplementary figure.

To quantify the effect of environmental variables and number of RTIs on the overall microbiota composition we performed permutational multivariate analysis of variance (PERMANOVA)-tests (*adonis* function of the *vegan* package; Bray-Curtis dissimilarity, 999 permutations). To assess the robustness of our findings based on one rarefied OTU-table, we reran the same PERMANOVA-tests on 100 rarefied OTU-tables and compared the effect size of the variables under consideration across rarefactions (Table E3A and E3C).

Clustering and alluvial diagram

To complement our findings based on our group-level analyses, we additionally assessed microbial development at the individual level. We first clustered individuals using unsupervised average linkage hierarchical clustering based on the Bray-Curtis dissimilarity matrix. The number of clusters was determined based on the Silhouette and Calinski-Harabasz indices (*fpc* package) (E21). Clusters consisting ≥10 samples were considered for subsequent analyses. The proportion of samples within each cluster at each time point was visualised using an alluvial diagram (*ggvisSankey*-function within the *googleVis* package) (E22).

The alluvial diagram was stratified into three groups based on the normal distribution of RTIs in the population; 39 children with 0-2 RTIs (reference group), 52 children with 3-4 RTIs and 21 children with 5-7 RTIs over the first year of life.

Random forest modelling

We hypothesized that the microbial succession patterns in the upper respiratory tract would be altered in children who are more susceptible to RTIs. To investigate this hypothesis, we used a machine learning technique referred to as random forest, which consists of an ensemble of decision trees, each of which is built based on random partition of the data, using a random selection of predictors (E23). We chose a random forest-approach over a more traditional, reductionist approach where we would model individual OTUs, as we did not want to make any assumptions on the highly variable relationships between specific OTUs and age (figure E7). Also, OTU-abundance data is usually very sparse and overdispersed, which hinders the application of traditional statistical techniques. Last, the random forest approach enabled us to simultaneously model these challenging data, as well as reduce the dimensionality of the data, the latter of which is essential to microbiota analysis.

To identify OTUs characteristic of a healthy microbiota maturation, we regressed the relative abundance of the 576 OTUs observed against chronological age in the reference group (i.e. 0-2 RTIs) using the *randomForest* package, (ntree=10,000, default mtry, defined as the number of variables in the model divided by 3) (E24), as previously described (E16). The optimal number of age-discriminatory taxa required for the prediction of microbiota age was determined by calculating the cross-validated prediction performance of models with a sequentially reduced numbers of variables (ranked by importance measured by the mean increase of squared error if that variable would be removed from the model; *caret* package (E25); 100 iterations; Figure E3A and E3B). This selection of OTUs was subsequently used as input to a random forest model used to regress the relative abundance versus chronological age in the reference group (resulting in the final model). We determined the importance of the reduced set of variables based on the percentage increase in mean squared error after permuting the values for each OTU (100 iterations). The final model was then used to predict chronological age, referred to

as 'microbiota age', in individuals who experienced 3-4 and 5-7 RTIs and on the group of samples collected during RTIs. We used the *train* function in the 'caret' package (E25) to determine cross-validated predictions of microbiota age for the healthy cohort (10 folds, 100 iterations, default mtry) to avoid reporting overfitted estimates (Figure 4A). The importance of the age-discriminatory OTUs was visualised per cohort at each time point using a heatmap. OTUs were vertically ordered based on an average linkage hierarchical clustering to visualise the interrelations between OTUs. The colours of the heatmap were row-wise normalized (i.e. red indicates the highest relative abundance of that OTU, black indicates the lowest value.). As a post-hoc analysis, we studied the effect of the *Moraxella*-genus on the performance of the microbiota age model by excluding the OTUs belonging to the *Moraxella*-genus from the model while monitoring the amount of variance explained.

Since the relationship between chronological age and microbiota age was not linear, we calculated the relative microbiota age as described before (E16). Relative microbiota age (RMA) was calculated as follows: relative microbiota age = microbiota age of a given child – microbiota age of children of similar age in the reference group (determined by a spline fit) (E16).

Linear mixed models

Linear mixed models were used to assess the effect of fixed variables on a continuous dependent variable, while including subject as a random intercept to adequately control for repeated measures (*lmer* function of the *lme4* package) (E26). Separate models were used study the effect of 1) environmental variables and 2) RTI susceptibility (defined as having experienced 0-2, 3-4 or 5-7 RTIs during the first year of life) on relative microbiota age, Bray-Curtis-dissimilarity and α-diversity measures. If a non-linear relationship between age and the dependent variable

was suspected, age was included in the model as a natural spline fit with five degrees of freedom (*ns* function of the *splines* R-package). In addition, we assessed influence of sampling moment on bacterial density (log_{10}-transformed) and relative abundance (only first four time points) using linear mixed models. Furthermore, we investigated the changes in RMA and the relative abundance of age-discriminatory taxa at two time points before RTI, during RTI and at one time point after RTI using a mixed linear model with RMA/OTU-abundance as outcome variables and including timing of sampling (i.e. '-2', '-1', 'RTI' or '+1'), age as fixed effects and subject as random effect. We did not consider interactions between variables in our models. Post-hoc tests on contrasts of interest were performed using the *multcomp* package (E27). Contrasts as specified in the main text were included and we adjusted for multiple testing using the 'single-step' procedure (*multcomp* default), except when stated otherwise.

Time series modelling

To assess differences in abundance of OTUs between groups, we used smoothing spline ANOVA as implemented in the *fitTimeSeries* function (E28) of the *metagenomeseq* R-package (E17), which aims to model the differences in OTU-abundances between groups over time and is able to not only test if differences exist, but also to evaluate the timing of these differences. In addition, this function allows for the inclusion of a 'class'-effect, to adequately control for repeated measures. Smoothing spline ANOVA models were used to study the (timing of) differential abundance of age-discriminatory taxa determined by random forest between children with 0-2 versus 3-4 RTIs and 0-2 versus 5-7 RTIs over the first year of life. In addition, these models were used to assess the effect of birth mode and exclusive breastfeeding until three months on the abundance of OTUs that passed the abundance filter, as these variables likely have a temporary effect on microbial abundance. P-values were determined based on 1,000 permutations.

Multivariable modelling

To identify significant associations between environmental variables (as defined before) and the relative abundance of OTUs in a multivariable manner, we used Multivariate Association with Linear Models (MaAsLin). Age was included as a natural spline with five degrees of freedom. Taxonomic entities simultaneously included in the models were OTUs that passed the abundance filtering criterion and OTUs binned together at higher taxonomic levels (i.e. genus, family, class, order, phylum and kingdom). We included subject as a random effect and ran the models using default settings.

References

E1. Delnord M, Blondel B, Drewniak N, Klungsøyr K, Bolumar F, Mohangoo A, Gissler M, Szamotulska K, Lack N, Nijhuis J, Velebil P, Sakkeus L, Chalmers J, Zeitlin J, Euro-Peristat Preterm Group. Varying gestational age patterns in cesarean delivery: an international comparison. *BMC Pregnancy Childbirth* 2014;14:321.

E2. Bosch AATM, Levin E, van Houten MA, Hasrat R, Kalkman G, Biesbroek G, de Steenhuijsen Piters WAA, de Groot P-KCM, Pernet P, Keijser BJF, Sanders EAM, Bogaert D. Development of Upper Respiratory Tract Microbiota in Infancy is Affected by Mode of Delivery. *EBioMedicine* 2016;9:336–345.

E3. Wyllie AL, Chu MLJN, Schellens MHB, van Engelsdorp Gastelaars J, Jansen MD, van der Ende A, Bogaert D, Sanders EAM, Trzciński K. Streptococcus pneumoniae in Saliva of Dutch Primary School Children. *PLoS ONE* 2014;9:e102045.

E4. Bogaert D, Keijser B, Huse S, Rossen J, Veenhoven R, van Gils E, Bruin J, Montijn R, Bonten M, Sanders E. Variability and diversity of nasopharyngeal microbiota in children: a metagenomic analysis. *PLoS ONE* 2011;6:e17035.

E5. Biesbroek G, Tsivtsivadze E, Sanders EAM, Montijn R, Veenhoven RH, Keijser BJF, Bogaert D. Early respiratory microbiota composition determines bacterial succession patterns and respiratory health in children. *Am J Respir Crit Care Med* 2014;190:1283–1292.

E6. Joshi NA, Fass JN. Sickle: A sliding-window, adaptive, quality-based trimming tool for FastQ files. 1st ed. at <https://github.com/najoshi/sickle.>.

E7. Nikolenko SI, Korobeynikov AI, Alekseyev MA. BayesHammer: Bayesian clustering for error correction in single-cell sequencing. *BMC Genomics* 2013;14 Suppl 1:S7.

E8. Masella AP, Bartram AK, Truszkowski JM, Brown DG, Neufeld JD. PANDAseq: paired-end assembler for illumina sequences. *BMC Bioinformatics* 2012;13:31.

E9. Schirmer M, Ijaz UZ, D'Amore R, Hall N, Sloan WT, Quince C. Insight into biases and sequencing errors for amplicon sequencing with the Illumina MiSeq platform. *Nucleic Acids Res* 2015;43:e37–e37.

E10. Caporaso JG, Kuczynski J, Stombaugh J, Bittinger K, Bushman FD, Costello EK, Fierer N, Peña AG, Goodrich JK, Gordon JI, Huttley GA, Kelley ST, Knights D, Koenig JE, Ley RE, Lozupone CA, McDonald D, Muegge BD, Pirrung M, Reeder J, Sevinsky JR, Turnbaugh PJ, Walters WA, Widmann J, Yatsunenko T, Zaneveld J, Knight R. QIIME allows analysis of high-throughput community sequencing data. *Nat Methods* 2010;7:335–336.

E11. Westcott SL, Schloss PD. De novo clustering methods outperform reference-based methods for assigning 16S rRNA gene sequences to operational taxonomic units. *PeerJ* 2015;3:e1487.

E12. Wang Q, Garrity GM, Tiedje JM, Cole JR. Naive Bayesian classifier for rapid assignment of rRNA sequences into the new bacterial taxonomy. *Appl Environ Microbiol* 2007;73:5261–5267.

E13. Claesson MJ, O'Sullivan O, Wang Q, Nikkilä J, Marchesi JR, Smidt H, de Vos WM, Ross RP, O'Toole PW. Comparative analysis of pyrosequencing and a phylogenetic microarray for exploring microbial community structures in the human distal intestine. *PLoS ONE* 2009;4:e6669.

E14. Quast C, Pruesse E, Yilmaz P, Gerken J, Schweer T, Yarza P, Peplies J, Glöckner FO. The SILVA ribosomal RNA gene database project: improved data processing and web-based tools. *Nucleic Acids Res* 2013;41:D590–6.

E15. Zhang Z, Schwartz S, Wagner L, Miller W. A greedy algorithm for aligning DNA sequences. *J Comput Biol* 2000;7:203–214.

E16. Subramanian S, Huq S, Yatsunenko T, Haque R, Mahfuz M, Alam MA, Benezra A, DeStefano J, Meier MF, Muegge BD, Barratt MJ, VanArendonk LG, Zhang Q, Province MA, Petri WA, Ahmed T, Gordon JI. Persistent gut microbiota immaturity in malnourished Bangladeshi children. *Nature* 2014;510:417–421.

E17. Paulson JN, Stine OC, Bravo HC, Pop M. Differential abundance analysis for microbial marker-gene surveys. *Nat Methods* 2013;10:1200–1202.

E18. Biesbroek G, Sanders EAM, Roeselers G, Wang X, Caspers MPM, Trzciński K, Bogaert D, Keijser BJF. Deep sequencing analyses of low density microbial communities: working at the boundary of accurate microbiota detection. *PLoS ONE* 2012;7:e32942.

E19. Yoshida K, Bohn J. tableone: Create “Table 1” to Describe Baseline Characteristics. 0 ed. 2015;at <https://CRAN.R-project.org/package=tableone>.

E20. Oksanen J, Blanchet FG, Kindt R, Legendre P, Minchin PR, O'Hara RB, Simpson GL, Solymos P, Stevens M, Wagner H. vegan: Community Ecology Package. 2015;at <http://CRAN.R-project.org/package=vegan>.

E21. Hennig C. fpc: Flexible Procedures for Clustering. 2015;at <http://CRAN.R-project.org/package=fpc>.

E22. Gesmann M, de Castillo D. Using the Google Visualisation API with R. *R Journal* 2011;3:40–44.

E23. Breiman L. Random forests. *Machine learning* 2001;

E24. Liaw A, Wiener M. Classification and Regression by randomForest. *R news* 2002;2:18–22.

E25. Kuhn M. Building Predictive Models in R Using the caret Package. *J Stat Softw* 2008;28:.

E26. Bates D, Mächler M, Bolker B, Walker S. Fitting Linear Mixed-Effects Models Using lme4. *J Stat Softw* 2015;67:.

E27. Hothorn T, Bretz F, Westfall P, Heiberger RM. Package “multcomp.” 2016;

E28. Talukder H, Paulson JN, Bravo HC. fitTimeSeries: Longitudinal differential abundance analysis for marker-gene surveys. *bioconductorjp*

382
383
384

Figure E1

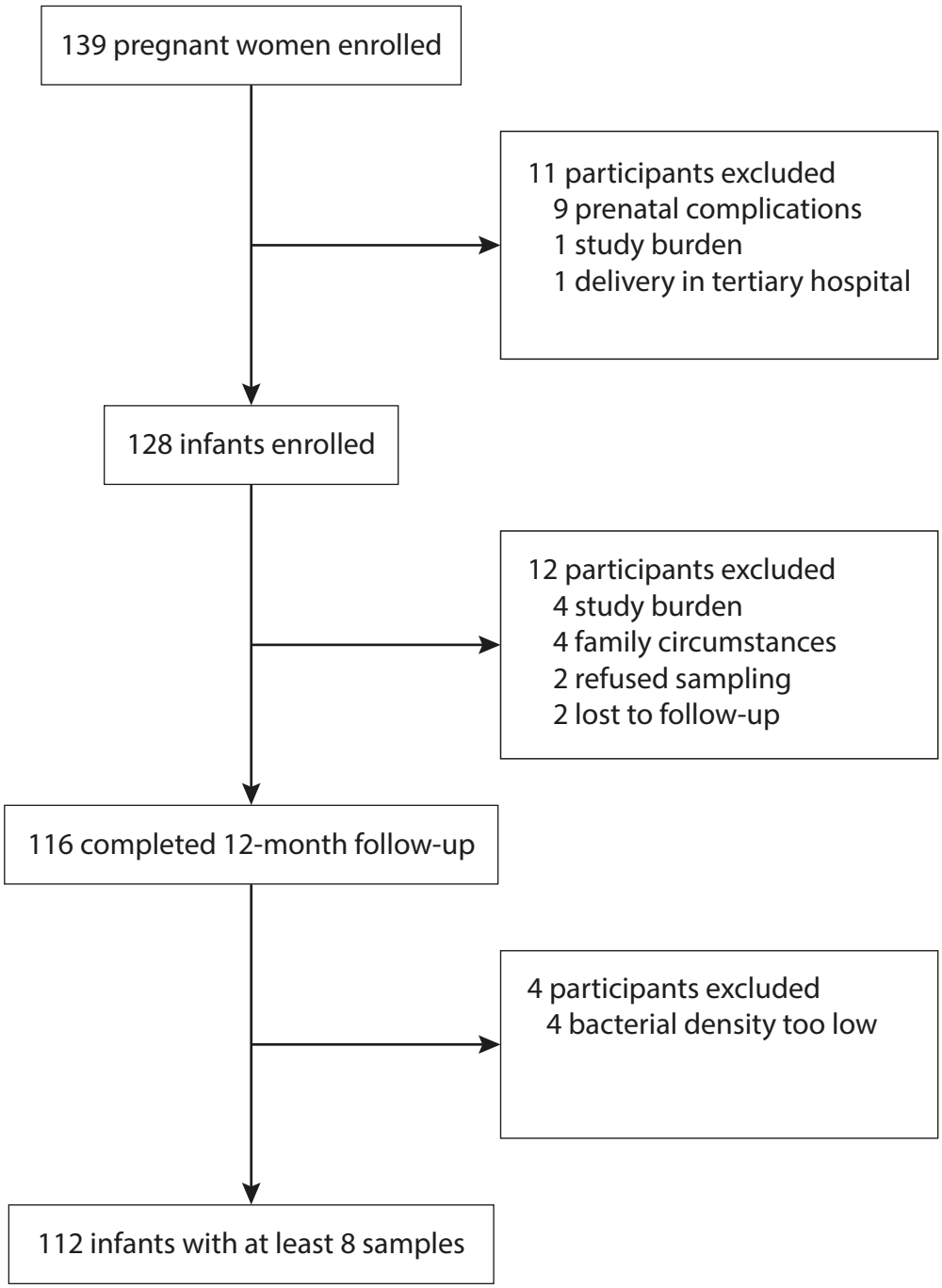
139 pregnant women enrolled
11 participants excluded
9 prenatal complications
1 study burden
1 delivery in tertiary hospital
128 infants enrolled
12 participants excluded
4 study burden
4 family circumstances
2 refused sampling
2 lost to follow-up
116 completed 12-month follow-up
4 participants excluded
4 bacterial density too low
112 infants with at least 8 samples

Figure E2

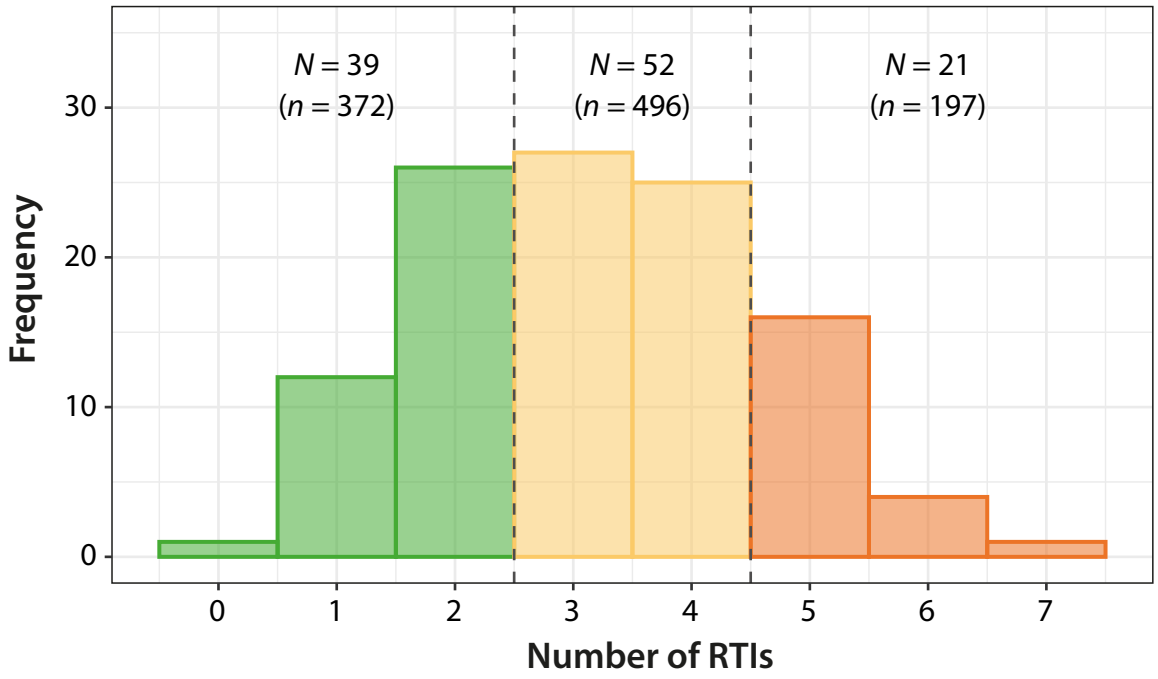
N = 39
(n = 372)
N = 52
(n = 496)
N = 21
(n = 197)
Frequency
30
20
10
0
0
1
2
3
4
5
6
7
Number of RTIs

Figure E3

A

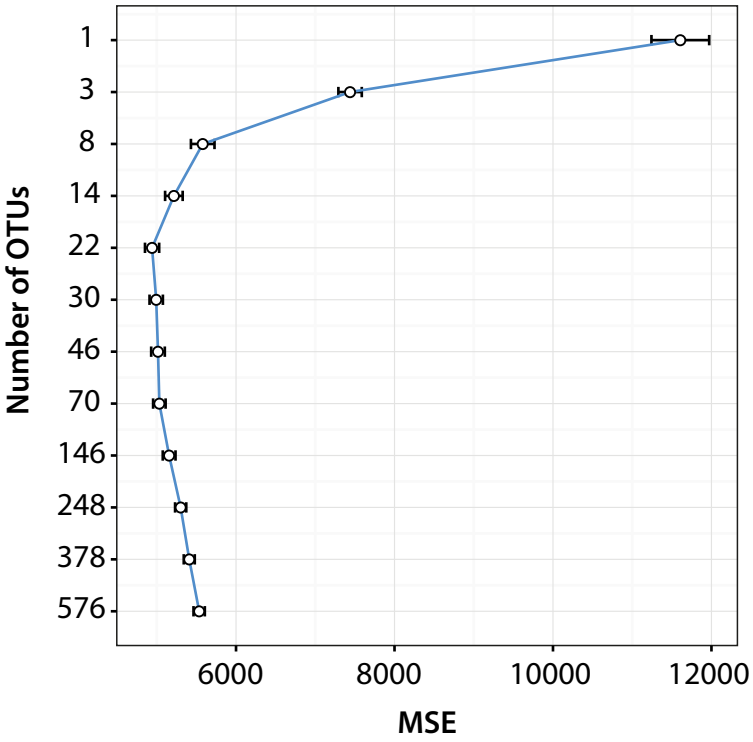
Number of OTUs
1
3
8
14
22
30
46
70
146
248
378
576
6000
8000
10000
12000
MSE

B

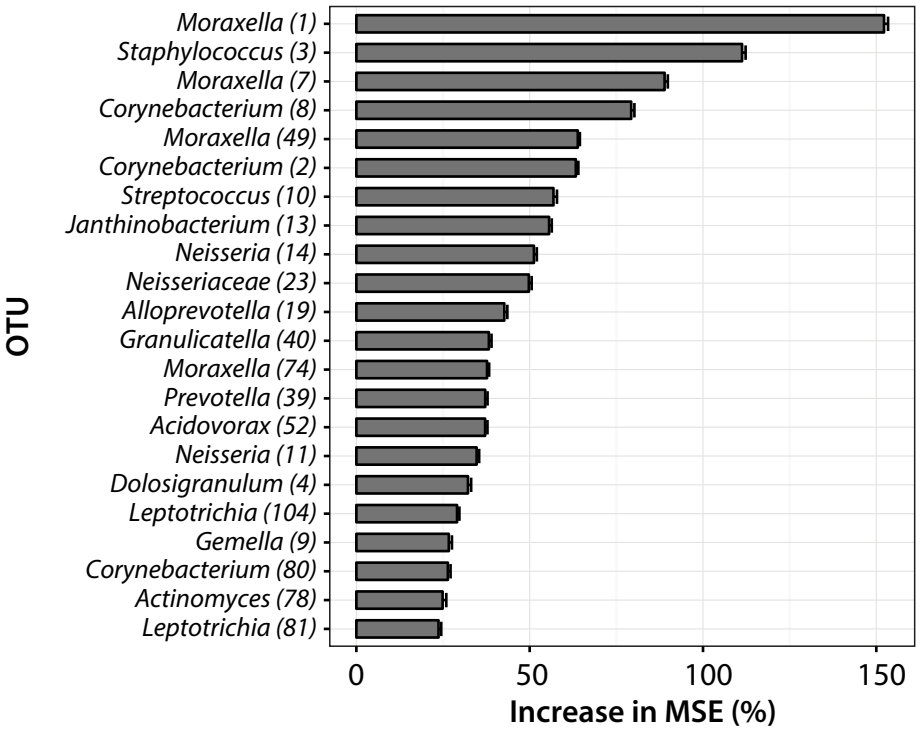
OTU
Moraxella (1)
Staphylococcus (3)
Moraxella (7)
Corynebacterium (8)
Moraxella (49)
Corynebacterium (2)
Streptococcus (10)
Janthinobacterium (13)
Neisseria (14)
Neisseriaceae (23)
Alloprevotella (19)
Granulicatella (40)
Moraxella (74)
Prevotella (39)
Acidovorax (52)
Neisseria (11)
Dolosigranulum (4)
Leptotrichia (104)
Gemella (9)
Corynebacterium (80)
Actinomyces (78)
Leptotrichia (81)
0
50
100
150
Increase in MSE (%)

Figure E4

A

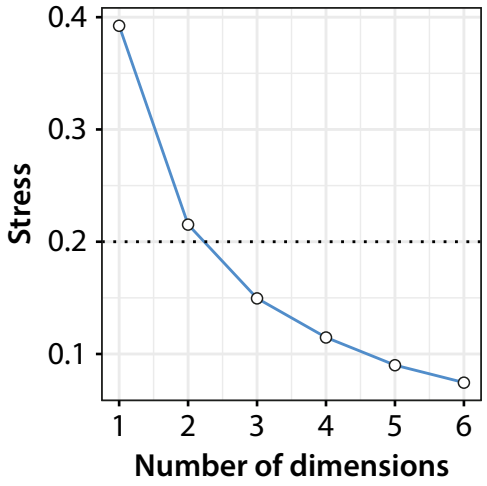
0.4
0.3
0.2
0.1
Stress
1
2
3
4
5
6
Number of dimensions

B

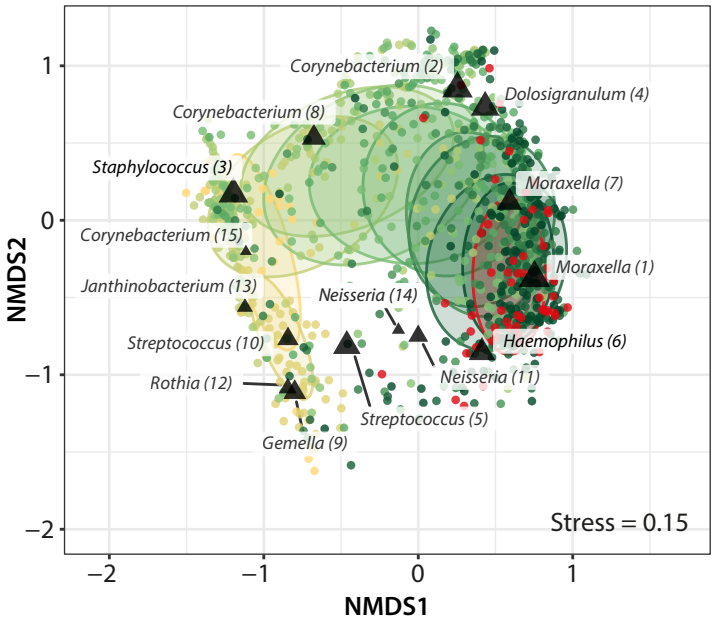
Corynebacterium (2)
Dolosigranulum (4)
Corynebacterium (8)
Staphylococcus (3)
Moraxella (7)
Corynebacterium (15)
Moraxella (1)
Janthinobacterium (13)
Neisseria (14)
Streptococcus (10)
Haemophilus (6)
Rothia (12)
Neisseria (11)
Streptococcus (5)
Gemella (9)
Stress = 0.15
NMDS1
NMDS2

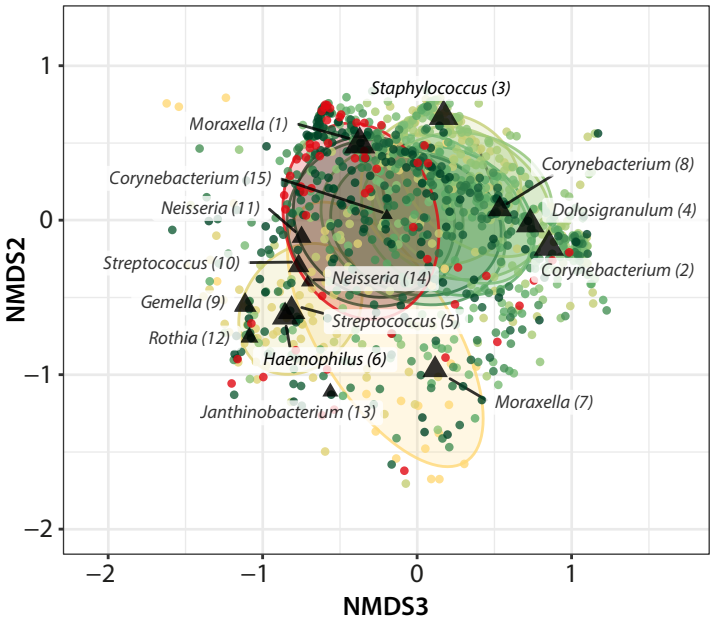
Staphylococcus (3)
Moraxella (1)
Corynebacterium (8)
Corynebacterium (15)
Dolosigranulum (4)
Neisseria (11)
Streptococcus (10)
Corynebacterium (2)
Neisseria (14)
Gemella (9)
Streptococcus (5)
Rothia (12)
Haemophilus (6)
Moraxella (7)
Janthinobacterium (13)
NMDS3
NMDS2

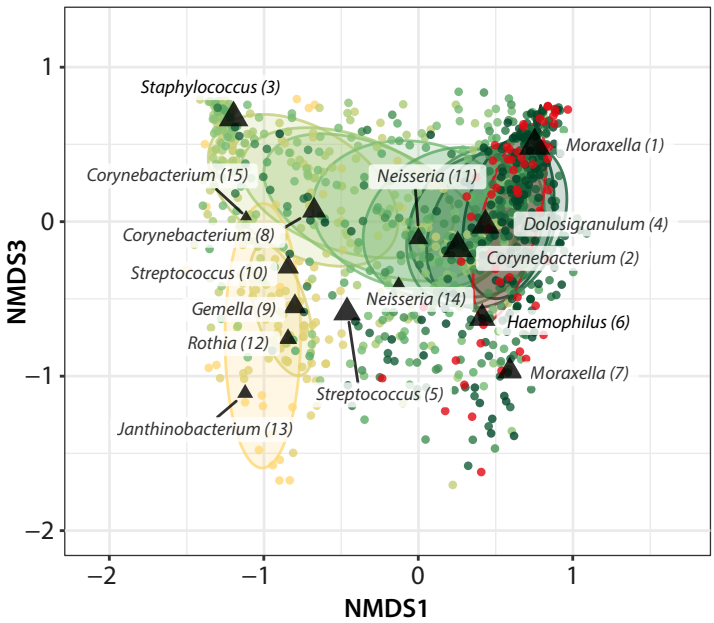
Staphylococcus (3)
Moraxella (1)
Corynebacterium (15)
Neisseria (11)
Dolosigranulum (4)
Corynebacterium (8)
Corynebacterium (2)
Streptococcus (10)
Neisseria (14)
Gemella (9)
Haemophilus (6)
Rothia (12)
Moraxella (7)
Streptococcus (5)
Janthinobacterium (13)
NMDS1
NMDS3

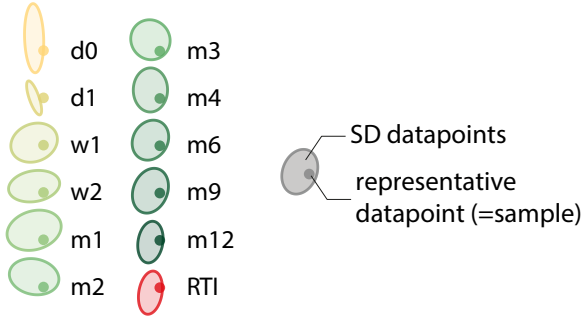
d0
d1
w1
w2
m1
m2
m3
m4
m6
m9
m12
RTI
SD datapoints
representative datapoint (=sample)

Figure E5

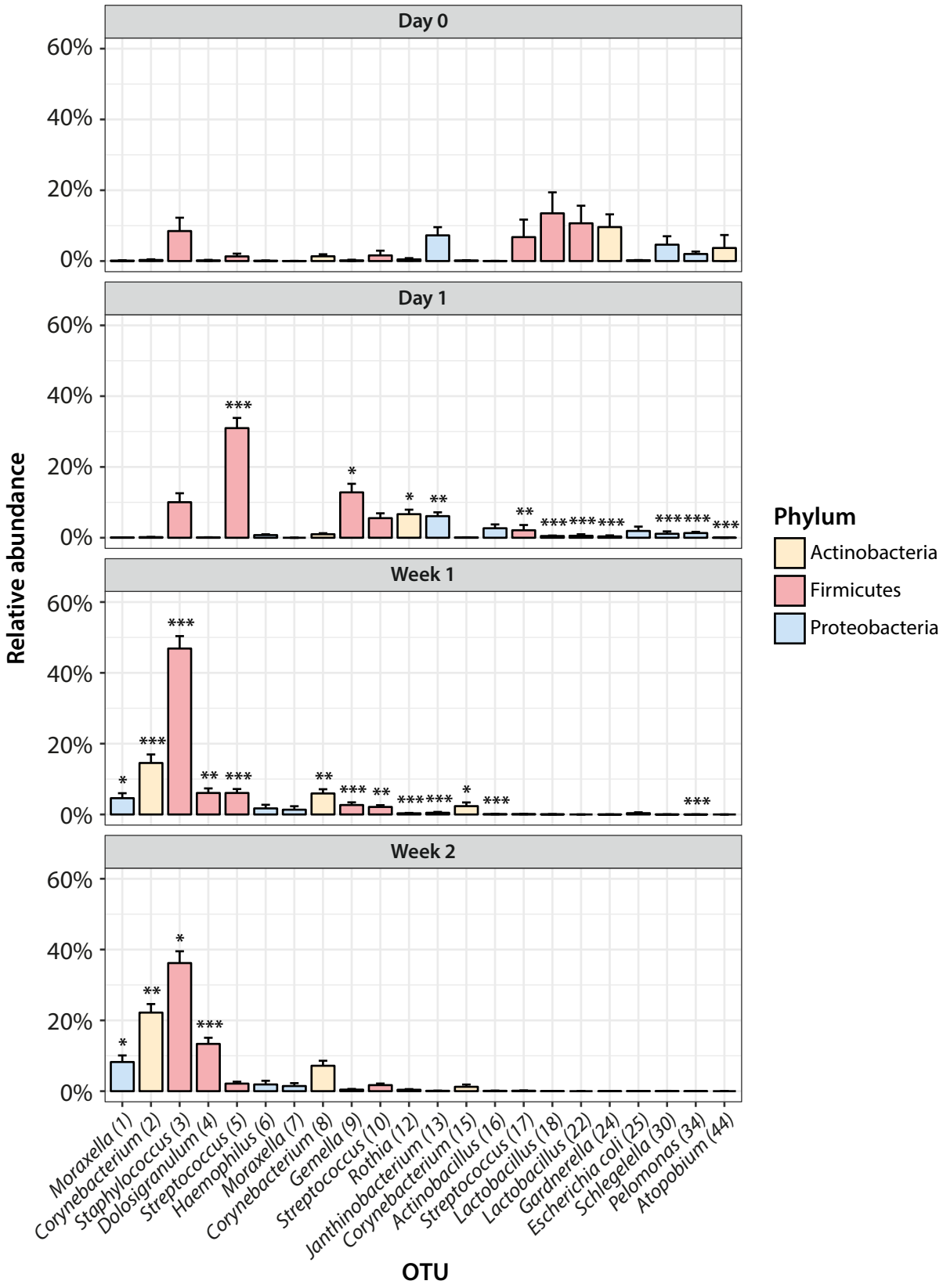
Day 0
Day 1
Week 1
Week 2
Relative abundance
60%
40%
20%
0%
Phylum
Actinobacteria
Firmicutes
Proteobacteria
OTU
Moraxella (1)
Corynebacterium (2)
Staphylococcus (3)
Dolosigranulum (4)
Streptococcus (5)
Haemophilus (6)
Moraxella (7)
Corynebacterium (8)
Gemella (9)
Streptococcus (10)
Rothia (12)
Janthinobacterium (13)
Corynebacterium (15)
Actinobacillus (16)
Streptococcus (17)
Lactobacillus (18)
Lactobacillus (22)
Gardnerella (24)
Escherichia coli (25)
Schlegelella (30)
Pelomonas (34)
Atopobium (44)

Figure E6

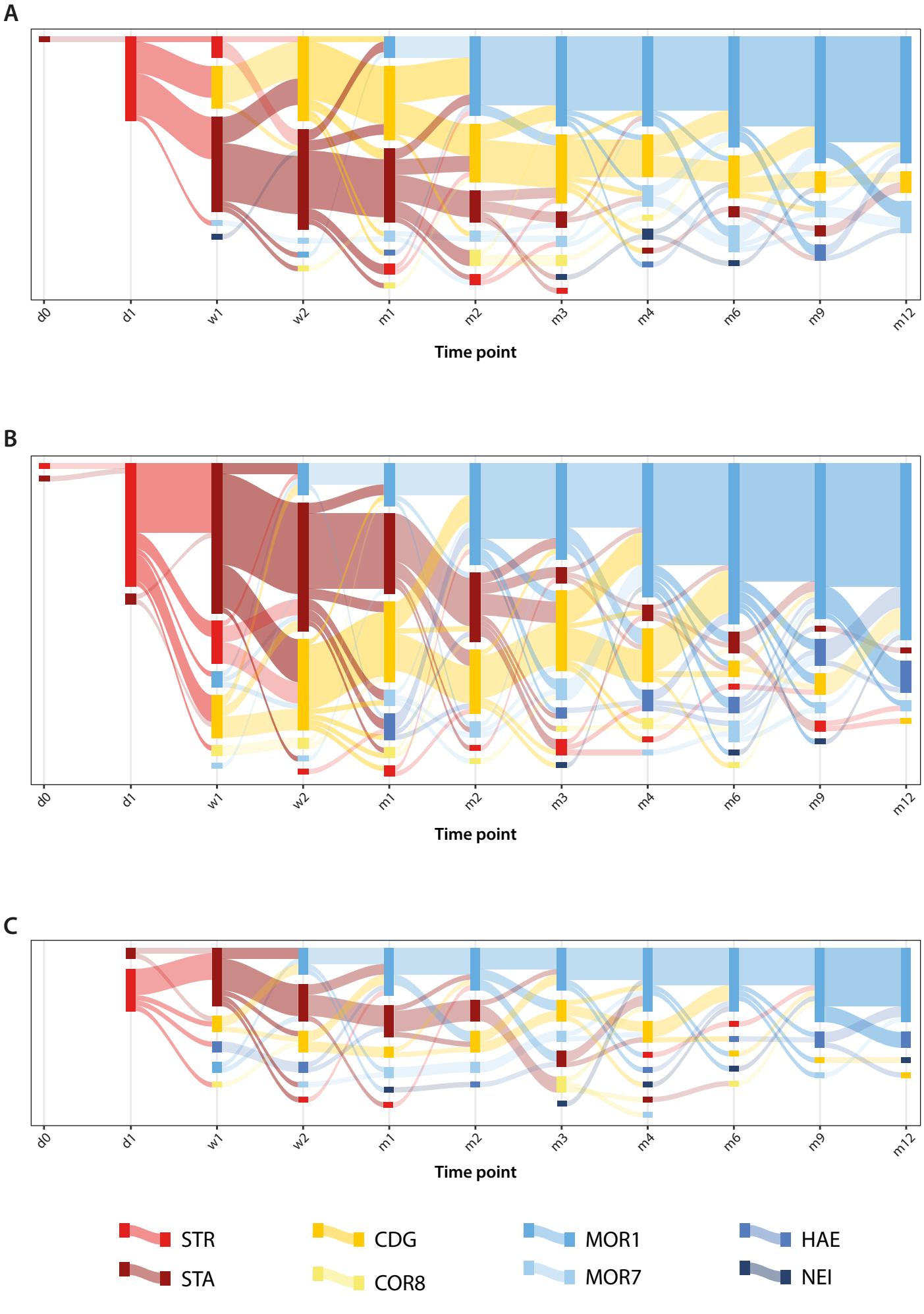
A
d0
d1
w1
w2
m1
m2
m3
m4
m6
m9
m12
Time point
B
d0
d1
w1
w2
m1
m2
m3
m4
m6
m9
m12
Time point
C
d0
d1
w1
w2
m1
m2
m3
m4
m6
m9
m12
Time point
STR
STA
CDG
COR8
MOR1
MOR7
HAE
NEI

Figure E7

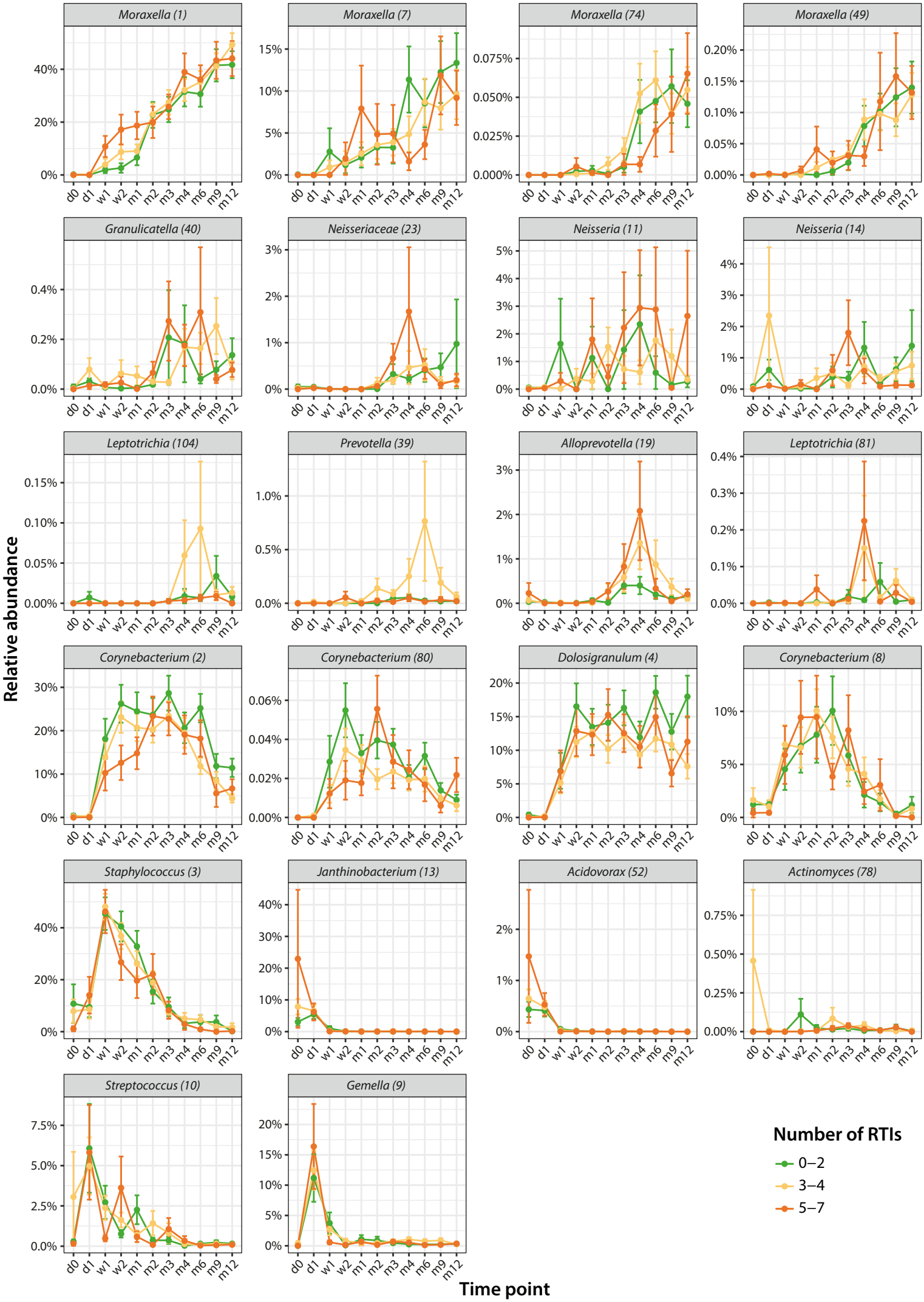
Moraxella (1)
Moraxella (7)
Moraxella (74)
Moraxella (49)
Granulicatella (40)
Neisseriaceae (23)
Neisseria (11)
Neisseria (14)
Leptotrichia (104)
Prevotella (39)
Alloprevotella (19)
Leptotrichia (81)
Corynebacterium (2)
Corynebacterium (80)
Dolosigranulum (4)
Corynebacterium (8)
Staphylococcus (3)
Janthinobacterium (13)
Acidovorax (52)
Actinomyces (78)
Streptococcus (10)
Gemella (9)
Relative abundance
Time point
d0 d1 w1 w2 m1 m2 m3 m4 m6 m9 m12
Number of RTIs
0–2
3–4
5–7

Figure E8

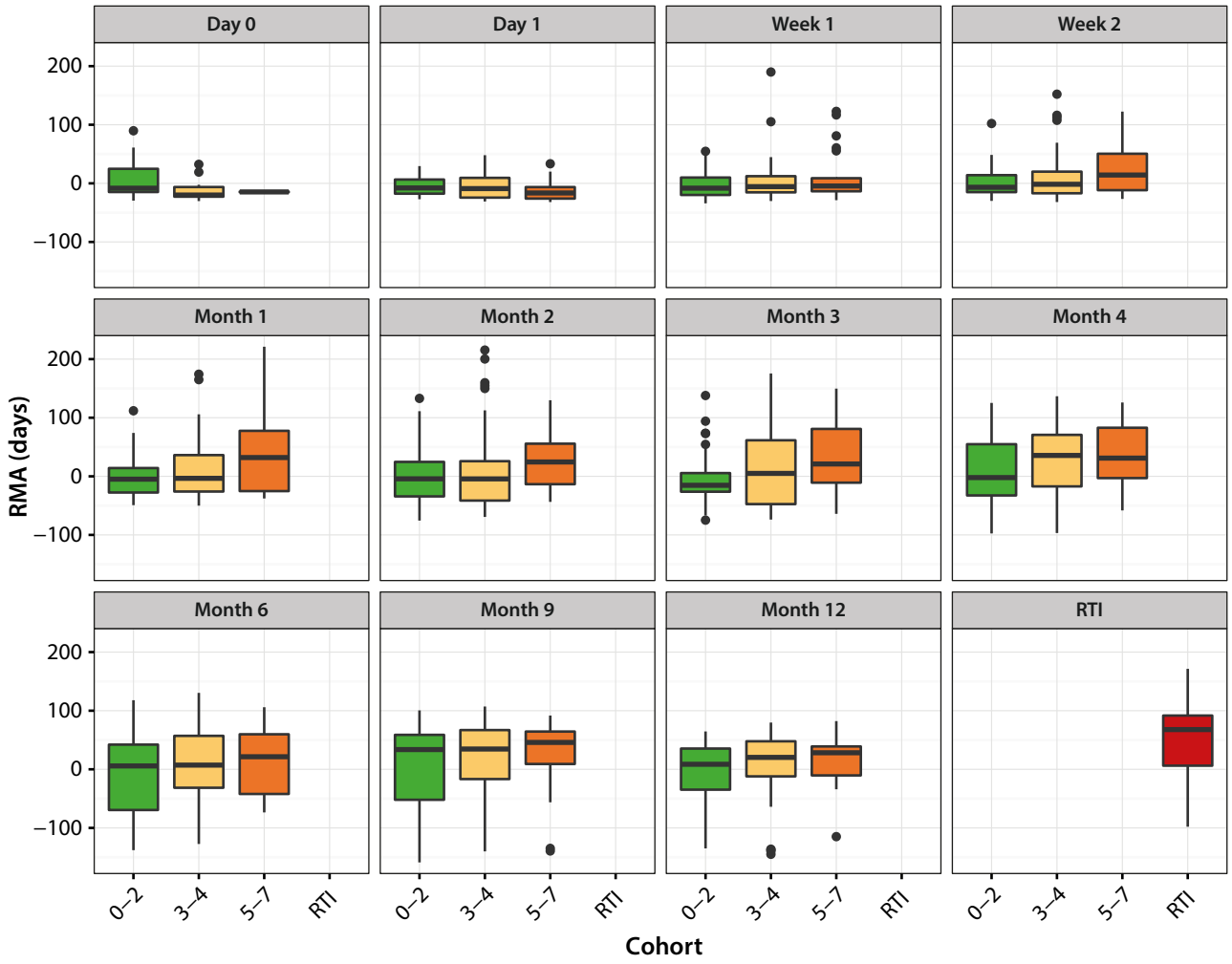
Day 0
Day 1
Week 1
Week 2
Month 1
Month 2
Month 3
Month 4
Month 6
Month 9
Month 12
RTI
RMA (days)
200
100
0
−100
0–2
3–4
5–7
RTI
Cohort

Figure E9

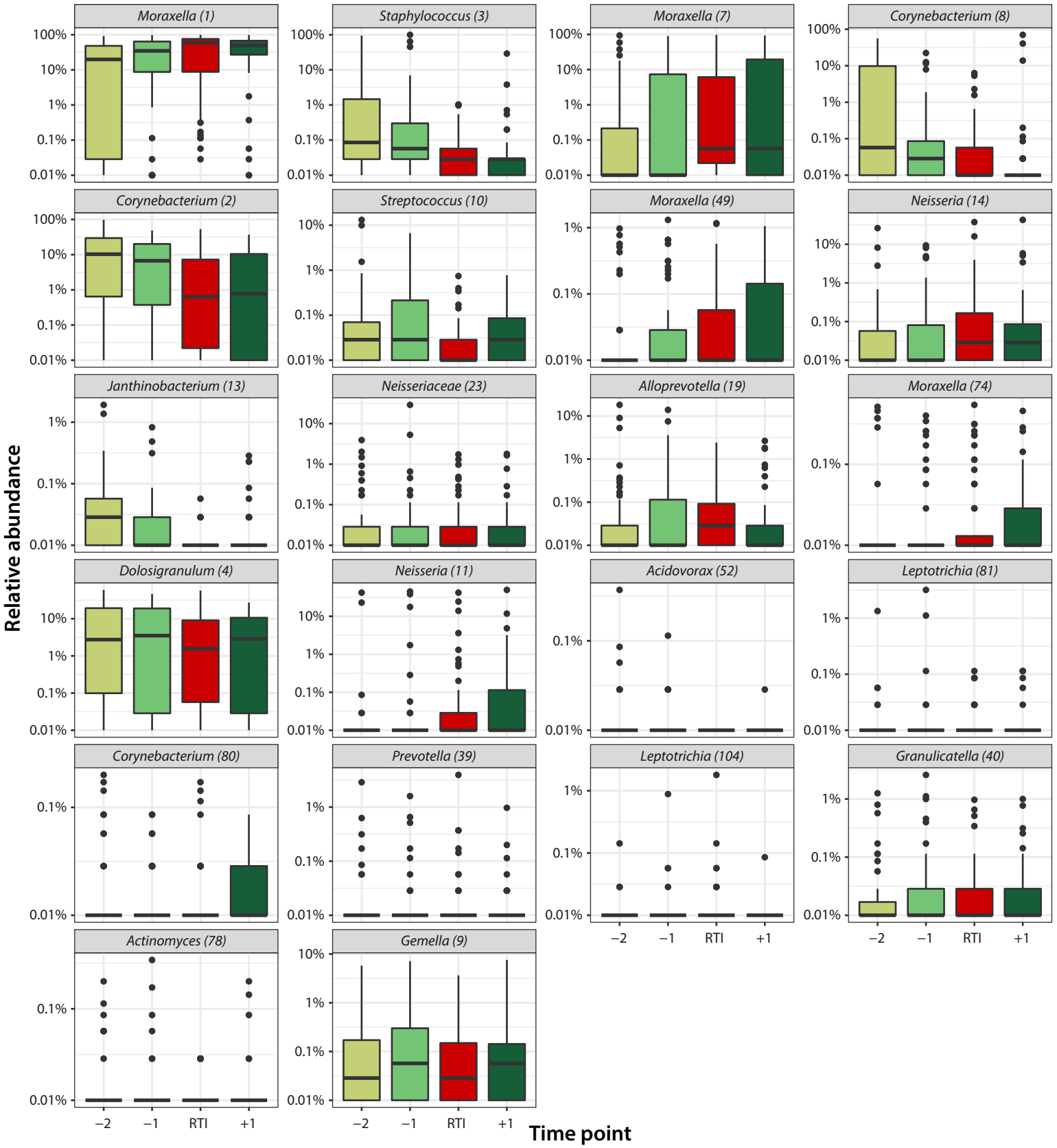
Moraxella (1)
Staphylococcus (3)
Moraxella (7)
Corynebacterium (8)
Corynebacterium (2)
Streptococcus (10)
Moraxella (49)
Neisseria (14)
Janthinobacterium (13)
Neisseriaceae (23)
Alloprevotella (19)
Moraxella (74)
Dolosigranulum (4)
Neisseria (11)
Acidovorax (52)
Leptotrichia (81)
Corynebacterium (80)
Prevotella (39)
Leptotrichia (104)
Granulicatella (40)
Actinomyces (78)
Gemella (9)
Relative abundance
100%
10%
1%
0.1%
0.01%
−2
−1
RTI
+1
Time point

Figure E10

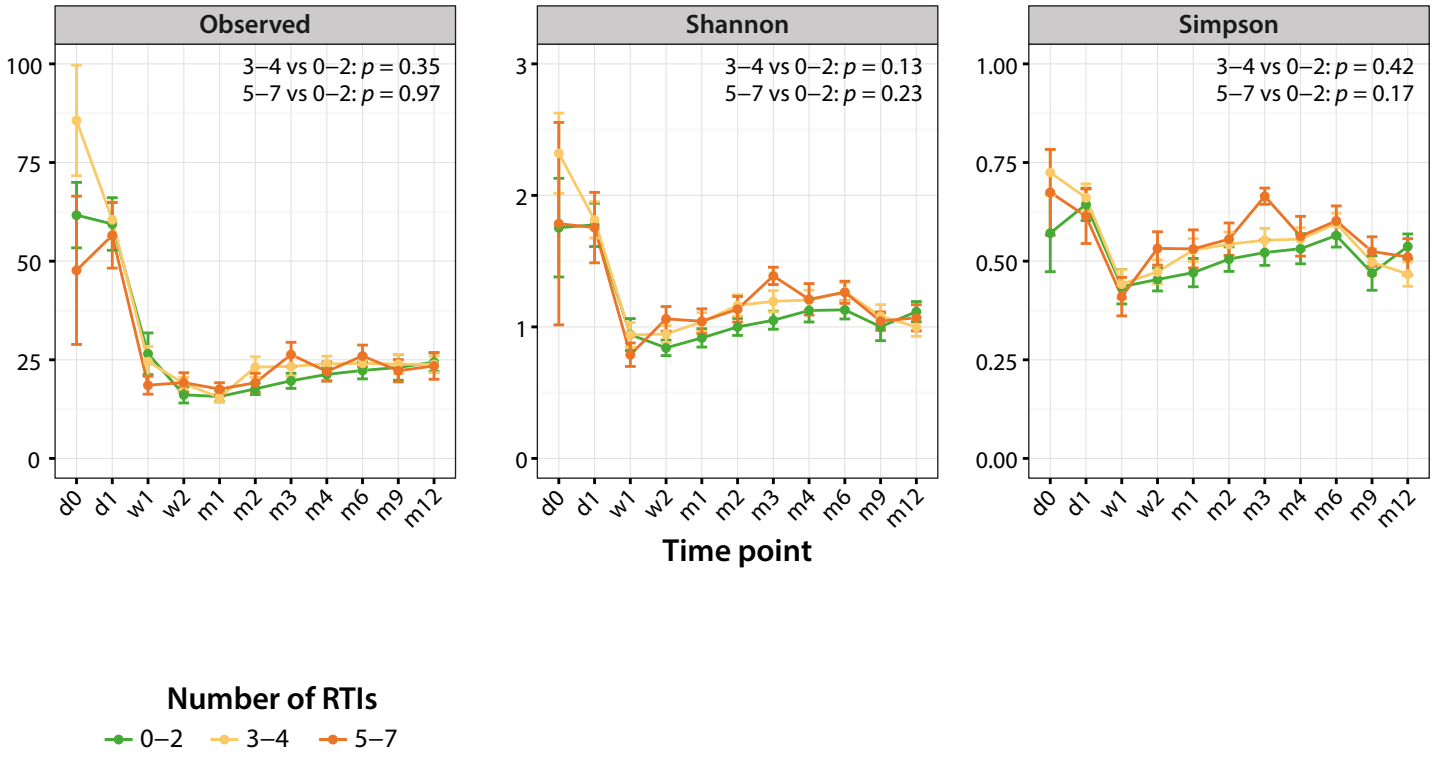
Observed
Shannon
Simpson
3–4 vs 0–2: p = 0.35
5–7 vs 0–2: p = 0.97
3–4 vs 0–2: p = 0.13
5–7 vs 0–2: p = 0.23
3–4 vs 0–2: p = 0.42
5–7 vs 0–2: p = 0.17
100
75
50
25
0
3
2
1
0
1.00
0.75
0.50
0.25
0.00
d0
d1
w1
w2
m1
m2
m3
m4
m6
m9
m12
Time point
Number of RTIs
0–2
3–4
5–7

Figure E11

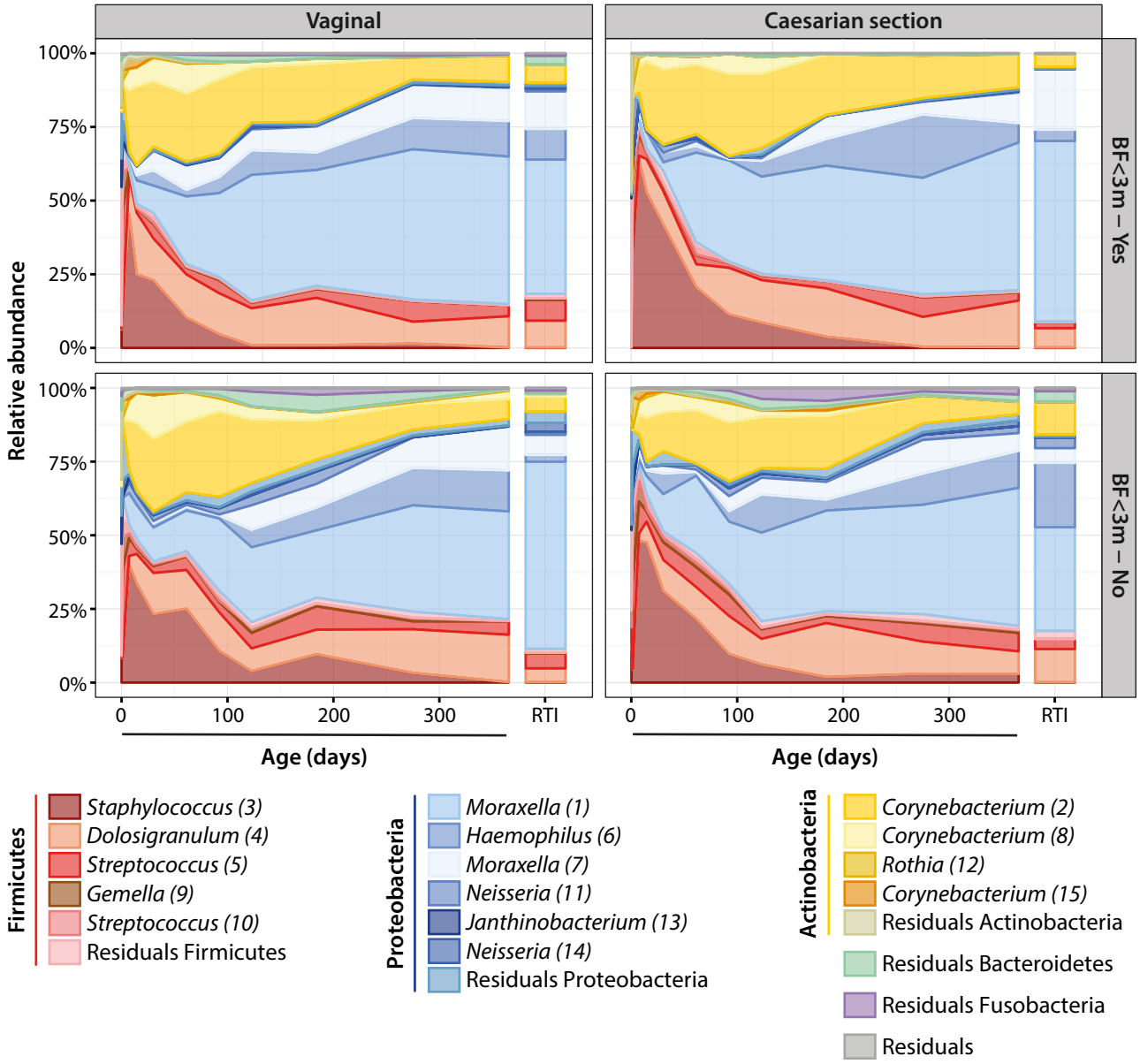
Vaginal
Caesarian section
BF<3m – Yes
BF<3m – No
Relative abundance
100%
75%
50%
25%
0%
0
100
200
300
RTI
Age (days)
Firmicutes
Staphylococcus (3)
Dolosigranulum (4)
Streptococcus (5)
Gemella (9)
Streptococcus (10)
Residuals Firmicutes
Proteobacteria
Moraxella (1)
Haemophilus (6)
Moraxella (7)
Neisseria (11)
Janthinobacterium (13)
Neisseria (14)
Residuals Proteobacteria
Actinobacteria
Corynebacterium (2)
Corynebacterium (8)
Rothia (12)
Corynebacterium (15)
Residuals Actinobacteria
Residuals Bacteroidetes
Residuals Fusobacteria
Residuals

Figure E12

A

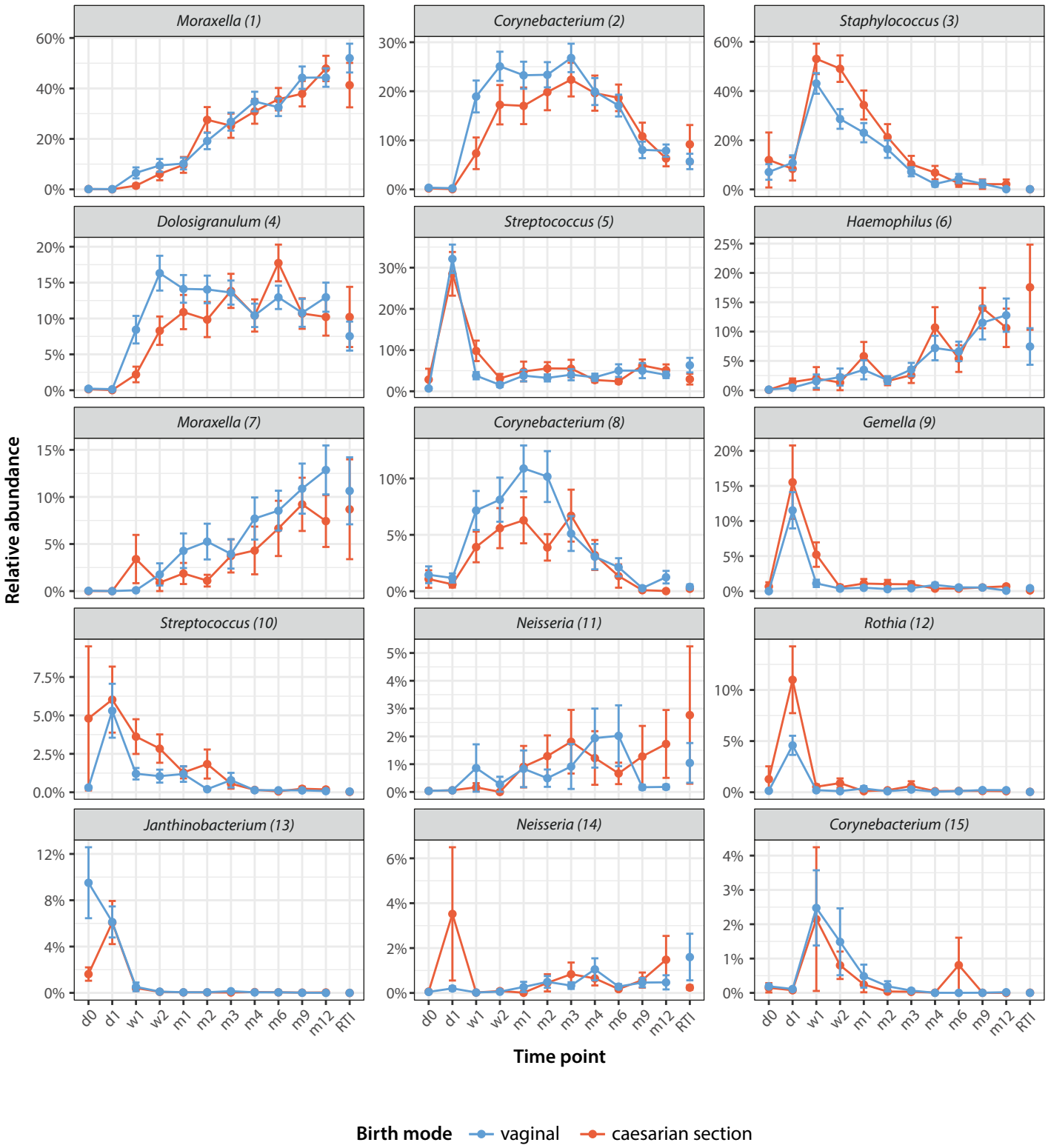
Moraxella (1)
Corynebacterium (2)
Staphylococcus (3)
Dolosigranulum (4)
Streptococcus (5)
Haemophilus (6)
Moraxella (7)
Corynebacterium (8)
Gemella (9)
Streptococcus (10)
Neisseria (11)
Rothia (12)
Janthinobacterium (13)
Neisseria (14)
Corynebacterium (15)
Relative abundance
d0 d1 w1 w2 m1 m2 m3 m4 m6 m9 m12 RTI
Time point
Birth mode
vaginal
caesarian section

Cont'd **Figure E12**

B